

AD \_\_\_\_\_

CONTRACT NO: DAMD17-93-C-3070

TITLE: X-RAY CRYSTALLOGRAPHIC STUDIES ON ACETYLCHOLINESTERASE  
AND ON ITS INTERACTION WITH ANTICHOLINESTERASE AGENTS

PRINCIPAL INVESTIGATORS: Israel Silman, Ph.D.  
Joel L. Sussman, Ph.D.

CONTRACTING ORGANIZATION: Weizmann Institute of Science  
Rehovot 76100, Israel

REPORT DATE: 24 Nov 94

TYPE OF REPORT: Midterm

PREPARED FOR: U.S. Army Medical Research and Materiel Command  
Fort Detrick, Frederick, MD 21702-5012

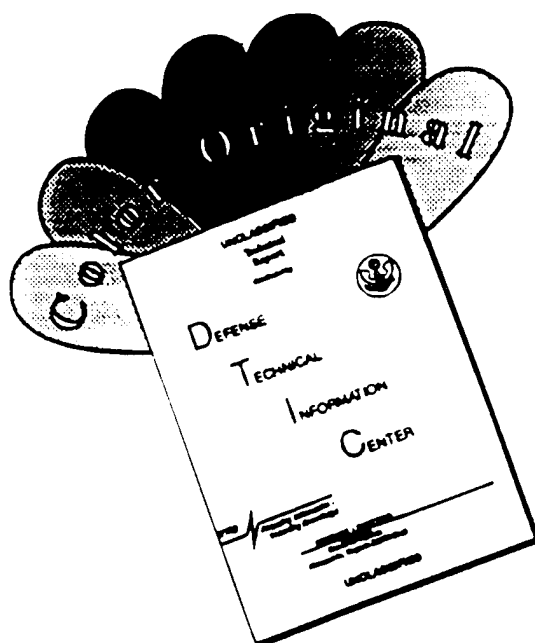
DISTRIBUTION STATEMENT: Approved for public release;  
distribution unlimited.

The findings in this report are not to be construed as an official Department of the Army position unless so designated by other authorized documents.

19960401 037

DTIC QUALITY INSPECTED 1

# DISCLAIMER NOTICE



THIS DOCUMENT IS BEST QUALITY AVAILABLE. THE COPY FURNISHED TO DTIC CONTAINED A SIGNIFICANT NUMBER OF COLOR PAGES WHICH DO NOT REPRODUCE LEGIBLY ON BLACK AND WHITE MICROFICHE.

REPORT DOCUMENTATION PAGE			Form Approved OMB No. 0704-0188	
Public reporting burden for this collection of information is estimated to average 1 hour per response, including the time for reviewing instructions, searching existing data sources, gathering and maintaining the data needed, and completing and reviewing the collection of information. Send comments regarding this burden estimate or any other aspect of this collection of information, including suggestions for reducing this burden, to Washington Headquarters Services, Directorate for Information Operations and Reports, 1215 Jefferson Davis Highway, Suite 1204, Arlington, VA 22202-4302, and to the Office of Management and Budget, Paperwork Reduction Project (0704-0188), Washington, DC 20503.				
1. AGENCY USE ONLY (Leave blank)		2. REPORT DATE 24 Nov 94		3. REPORT TYPE AND DATES COVERED Midterm, 30 Apr 93 - 29 Apr 94
4. TITLE AND SUBTITLE X-Ray Crystallographic Studies on Acetylcholinesterase and on its Interaction with Anticholinesterase Agents			5. FUNDING NUMBERS Contract No. DAMD17-93-C-3070	
6. AUTHOR(S) Israel Silman, Ph.D. Joel L. Sussman, Ph.D.				
7. PERFORMING ORGANIZATION NAME(S) AND ADDRESS(ES) Weizmann Institute of Science  Rehovot 76100 Israel			8. PERFORMING ORGANIZATION REPORT NUMBER	
9. SPONSORING/MONITORING AGENCY NAME(S) AND ADDRESS(ES) U.S. Army Medical Research and Materiel Command Fort Detrick, Frederick, MD 21702-5012			10. SPONSORING/MONITORING AGENCY REPORT NUMBER	
11. SUPPLEMENTARY NOTES				
12a. DISTRIBUTION/AVAILABILITY STATEMENT Approved for public release, distribution unlimited			12b. DISTRIBUTION CODE	
13. ABSTRACT (Maximum 200 words)  The EMBL-DESY synchrotron facility at Hamburg was employed to collect a complete 2.3 Å data set for a crystal of native <i>Torpedo</i> AChE, as well as for complexes with reversible ligands, including edrophonium, <i>d</i> -tubocurarine and huperzine A, diffracting to similar resolution. The X26c Laue beam line at the NSLS synchrotron facility at Brookhaven National Laboratory (BNL) was used to obtain a Laue diffraction pattern for a crystal of native <i>Torpedo</i> AChE, diffracting out to 2.8 Å. This is a first step towards our long-range objective of performing time-resolved X-ray crystallographic measurements on AChE. A complete 2.8 Å data set was collected on a covalent adduct of <i>Torpedo</i> AChE with the transition-state analog, <i>m</i> -( <i>N,N,N</i> -trimethylammonio) trifluoroacetophenone, which serves as a powerful, quasi-irreversible inhibitor. This permitted detailed analysis of the multiple ligand-AChE interactions.				
14. SUBJECT TERMS acetylcholinesterase; butyrylcholinesterase; Laue crystallography; synchrotron radiation; transition state analog; X-ray crystallography			15. NUMBER OF PAGES 43	
			16. PRICE CODE	
17. SECURITY CLASSIFICATION OF REPORT Unclassified	18. SECURITY CLASSIFICATION OF THIS PAGE Unclassified	19. SECURITY CLASSIFICATION OF ABSTRACT Unclassified	20. LIMITATION OF ABSTRACT Unlimited	

## GENERAL INSTRUCTIONS FOR COMPLETING SF 298

The Report Documentation Page (RDP) is used in announcing and cataloging reports. It is important that this information be consistent with the rest of the report, particularly the cover and title page. Instructions for filling in each block of the form follow. It is important to *stay within the lines* to meet *optical scanning requirements*.

**Block 1. Agency Use Only (Leave blank).**

**Block 2. Report Date.** Full publication date including day, month, and year, if available (e.g. 1 Jan 88). Must cite at least the year.

**Block 3. Type of Report and Dates Covered.** State whether report is interim, final, etc. If applicable, enter inclusive report dates (e.g. 10 Jun 87 - 30 Jun 88).

**Block 4. Title and Subtitle.** A title is taken from the part of the report that provides the most meaningful and complete information. When a report is prepared in more than one volume, repeat the primary title, add volume number, and include subtitle for the specific volume. On classified documents enter the title classification in parentheses.

**Block 5. Funding Numbers.** To include contract and grant numbers; may include program element number(s), project number(s), task number(s), and work unit number(s). Use the following labels:

<b>C</b> - Contract	<b>PR</b> - Project
<b>G</b> - Grant	<b>TA</b> - Task
<b>PE</b> - Program Element	<b>WU</b> - Work Unit Accession No.

**Block 6. Author(s).** Name(s) of person(s) responsible for writing the report, performing the research, or credited with the content of the report. If editor or compiler, this should follow the name(s).

**Block 7. Performing Organization Name(s) and Address(es).** Self-explanatory.

**Block 8. Performing Organization Report Number.** Enter the unique alphanumeric report number(s) assigned by the organization performing the report.

**Block 9. Sponsoring/Monitoring Agency Name(s) and Address(es).** Self-explanatory.

**Block 10. Sponsoring/Monitoring Agency Report Number.** (If known)

**Block 11. Supplementary Notes.** Enter information not included elsewhere such as: Prepared in cooperation with...; Trans. of...; To be published in.... When a report is revised, include a statement whether the new report supersedes or supplements the older report.

**Block 12a. Distribution/Availability Statement.** Denotes public availability or limitations. Cite any availability to the public. Enter additional limitations or special markings in all capitals (e.g. NOFORN, REL, ITAR).

**DOD** - See DoDD 5230.24, "Distribution Statements on Technical Documents."

**DOE** - See authorities.

**NASA** - See Handbook NHB 2200.2.

**NTIS** - Leave blank.

**Block 12b. Distribution Code.**

**DOD** - Leave blank.

**DOE** - Enter DOE distribution categories from the Standard Distribution for Unclassified Scientific and Technical Reports.

**NASA** - Leave blank.

**NTIS** - Leave blank.

**Block 13. Abstract.** Include a brief (*Maximum 200 words*) factual summary of the most significant information contained in the report.

**Block 14. Subject Terms.** Keywords or phrases identifying major subjects in the report.

**Block 15. Number of Pages.** Enter the total number of pages.

**Block 16. Price Code.** Enter appropriate price code (*NTIS only*).

**Blocks 17. - 19. Security Classifications.** Self-explanatory. Enter U.S. Security Classification in accordance with U.S. Security Regulations (i.e., UNCLASSIFIED). If form contains classified information, stamp classification on the top and bottom of the page.

**Block 20. Limitation of Abstract.** This block must be completed to assign a limitation to the abstract. Enter either UL (unlimited) or SAR (same as report). An entry in this block is necessary if the abstract is to be limited. If blank, the abstract is assumed to be unlimited.

## Abstract - continued

The X12c beam line at the BNL-NSLS synchrotron facility was used to collect an almost complete 2.8 Å data set for a conjugate of *Torpedo* AChE with the organophosphate inhibitor, paraoxon.

Highly purified preparations of HrAChE, expressed in human kidney cells, in which either monomeric or tetrameric molecular forms were predominant, were obtained by affinity chromatography followed by gel filtration.

A variety of crystallization conditions were screened for the HrAChE mentioned above, for purified HrAChE expressed in *E. coli*, for AChE purified from the venom of *Bungarus fasciatus* and for butyrylcholinesterase (BChE) purified from horse serum. Microcrystals were obtained for the HrAChE expressed in mammalian cells, for the snake venom enzyme and for horse serum BChE, and a diffraction pattern was obtained for the snake venom AChE.

Theoretical calculations show that AChE is characterized by a unique, asymmetric charge distribution resulting in an unusually high dipole moment. This dipole moment is oriented along the axis of the 'aromatic gorge' and its polarity is such that the positive substrate, ACh, would be attracted into the gorge.

Molecular dynamics simulations indicate that a polypeptide sequence, containing W84, near the bottom of the gorge, displays movements which might lead to transient opening of a 'back door' to the aromatic gorge. Existence of such a 'back door' might help explain traffic of substrate, solute and products through the gorge.

## FOREWORD

Options, interpretations, conclusions and recommendations are those of the author and are not necessarily endorsed by the U.S. Army.

\_\_\_\_\_ Where copyrighted material is quoted, permission has been obtained to use such material.

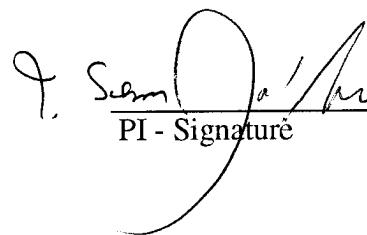
\_\_\_\_\_ Where material from documents designed for limited distribution is quoted, permission has been obtained to use the material.

\_\_\_\_\_ Citations of commercial organizations and trade names in this report do not constitute an official Department of the Army endorsement or approval of the products or services of these organizations.

\_\_\_\_\_ In conducting research using animals, the investigator(s) adhered to the "Guide for the Care and Use of Laboratory Animals," prepared by the Committee on Care and Use of Laboratory Animals of the Institute of Laboratory Resources, National Research Council (NIH Publication No. 86-23, Revised 1985).

\_\_\_\_\_ For the protection of human subjects, the investigator(s) adhered to policies of applicable Federal Law 45 CFR 46.

\_\_\_\_\_ In conducting research utilizing recombinant DNA technology, the investigator(s) adhered to current guidelines promulgated by the National Institutes of Health.

 3-21-90  
PI - Signature      DATE

## SUMMARY

The principal objectives of the current project included

1. Attempts to obtain crystals of acetylcholinesterase (AChE) other than of the enzyme from *Torpedo californica*, in particular of AChE of human origin.
2. Collection of improved data sets, viz. at higher resolution than previously, for crystals of *Torpedo* AChE.
3. Determination of the structure of complexes of *Torpedo* AChE with various ligands, including organophosphates.

In the first year of this project, we have made progress towards all three objectives, as well as in additional areas related to the long-term aims of our research program, as follows:

- A. We have obtained, by affinity chromatography followed by gel filtration, highly purified preparations of human recombinant AChE (HrAChE) expressed in human kidney cells in which either monomeric or tetrameric molecular forms were predominant.
- B. We have screened a variety of crystallization conditions for the HrAChE mentioned above, for purified preparations of HrAChE expressed in *E. coli*, of AChE purified from the venom of *Bungarus fasciatus*, and of butyrylcholinesterase (BChE) purified from horse serum. Microcrystals have been obtained for the HrAChE expressed in mammalian cells, for the snake venom enzyme and for horse serum BChE.
- C. A complete data set, to 2.8 Å, was collected for a covalent complex of *Torpedo* AChE with the transition-state analog, *m*-(*N,N,N*-trimethylammonio)trifluoroacetophenone (TMTFA), which serves as a powerful, quasi-irreversible inhibitor. This permitted a detailed analysis of the multiple interactions of the ligand and the protein, thus heightening our understanding of the structural factors governing specificity and catalytic potency.
- D. The EMBL-DESY synchrotron facility at Hamburg was employed to collect a complete data set for a crystal of native *Torpedo* AChE which diffracted out to 2.3 Å, as well as for complexes

with reversible anticholinesterase ligands, including edrophonium (EDR) and the alkaloids *d*-tubocurarine and huperzine A, diffracting to a similar resolution.

- E. The X12c beam line at the National Synchrotron Light Source (NSLS) facility at Brookhaven National Laboratory (BNL), was used to collect an almost complete data set, out to 2.8 Å, for a covalent complex of *Torpedo* AChE with the organophosphate inhibitor, paraoxon.
- F. The X26c Laue beam line at the NSLS synchrotron facility at BNL was used to obtain a Laue diffraction pattern for a crystal of native *Torpedo* AChE, diffracting out to 2.8 Å. This is a first step towards our long-range objective of performing time-resolved X-ray crystallographic measurements on AChE so as to gain a detailed picture of the structural features governing its reaction mechanism.
- G. Theoretical calculations show that AChE is characterized by a unique, asymmetric charge distribution which results in an unusually high dipole moment. This dipole moment is oriented along the axis of the 'aromatic gorge' and its polarity is such that the positive substrate, ACh, would be attracted into the gorge.
- H. Molecular dynamics simulations indicate that a polypeptide sequence, containing W84, near the bottom of the gorge, displays movements which might lead to transient opening of a 'back door' to the aromatic gorge. Existence of such a 'back door' might help to explain traffic of substrate, solute and products through the gorge.



## TABLE OF CONTENTS

I)	OBJECTIVES.....	6
II)	BACKGROUND.....	7
III)	RESULTS.....	10
	A) Acetylcholinesterase from <i>Torpedo californica</i> .....	10
	1) Native enzyme and non-covalently bound inhibitor complexes.....	10
	2) Transition-state analog-AChE complex.....	11
	3) Organophosphoryl-AChE conjugates.....	13
	B) Human Recombinant AChE.....	13
	1) HrAChE expressed in <i>Escherichia coli</i> .....	14
	2) HrAChE expressed in 293 cells.....	14
	C) <i>Bungarus fasciatus</i> AChE.....	15
	D) Horse serum BChE.....	16
	E) Theoretical Studies.....	16
	1) Electrostatic properties of AChE.....	16
	2) Structure and dynamics of the active site gorge.....	17
IV)	LIST OF FIGURES	
	Fig. 1A Diffraction pattern of a native <i>T. californica</i> AChE crystal.....	19
	Fig. 1B Precession photograph of a native <i>T. californica</i> AChE crystal.....	20
	Fig. 2A Laue diffraction pattern for an orthorhombic crystal of <i>Torpedo</i> AChE.....	21
	Fig. 2B Overlay of observed and simulated Laue diffraction patterns.....	22
	Fig. 3 Stereo omit map of the refined structure of the TMTFA-AChE complex.....	23
	Fig. 4 Hydrogen bonds and close distances between TMTFA and AChE.....	24
	Fig. 5 Sucrose gradient centrifugation of affinity-purified HrAChE.....	25
	Fig. 6 Gel filtration of affinity-purified HrAChE on a Sephacryl S-300 column.....	26
	Fig. 7 Sucrose gradient centrifugation of the peaks separated on the Sephacryl S-300 column.....	27
	Fig. 8 SDS-PAGE of affinity-purified HrAChE before and after gel filtration.....	28
	Fig. 9 Crystals of monomeric HrAChE.....	29
	Fig. 10 Diffraction pattern of <i>Bungarus fasciatus</i> AChE crystals.....	30
	Fig. 11 Crystals of horse serum BChE.....	31
	Fig. 12 Backbone drawing of AChE with electrostatic isopotential surfaces superimposed.....	32
	Fig. 13 Cross section through the active-site gorge of AChE.....	33
	Fig. 14 Ray-trace image of the active-site gorge <i>Torpedo</i> AChE.....	34
V)	REFERENCES.....	35

## I) OBJECTIVES

The overall objectives of this proposal are to better understand the catalytic mechanism of AChE and to characterize its various ligand binding sites. These objectives will be approached by the method of single crystal X-ray diffraction together with computational molecular model building. The project will involve the following principal topics:

- A. Data collection and structural refinement of complexes of *Torpedo* AChE with covalent and non-covalent AChE inhibitors of basic, pharmacological and toxicological importance.
- B. Attempts to crystallize human and bovine AChE and also horse serum BChE.
- C. Improved refinement of the structure of native *Torpedo* AChE.
- D. Synchrotron radiation X-ray data collection of *Torpedo* AChE.
- E. Homology model building of human and bovine fetal serum AChE.
- F. Model building of AChE-ligand conjugates.
- G. Prediction of targets for site-directed mutagenesis of AChE.

## II) BACKGROUND

The principal biological role of acetylcholinesterase (AChE) is believed to be termination of impulse transmission at cholinergic synapses by rapid hydrolysis of the neurotransmitter acetylcholine (ACh) (1). AChE is, accordingly, characterized by a remarkably high turnover, especially for a serine hydrolase, functioning at a rate approaching that of a diffusion-controlled reaction (2). The powerful acute toxicity of organophosphate poisons (as well as of carbamates and sulfonyl halides which function analogously) is attributed primarily to the fact that they are potent inhibitors of AChE (3). Inhibition is achieved by their covalent attachment to a serine residue within the active site (2, 4). AChE inhibitors have been used in the treatment of various diseases, such as myasthenia gravis and glaucoma (5) and, recently, are under active consideration for use in the management of Alzheimer's disease (6). Knowledge of the three-dimensional structure of AChE is, therefore, of fundamental interest for understanding its remarkable catalytic efficiency, and of applied importance in developing therapeutic approaches to organophosphate poisoning and in structure-related drug design. Furthermore, information concerning the ACh-binding site of AChE is also pertinent to an understanding of the molecular basis for the recognition of ACh by other ACh-binding proteins such as the various ACh receptors (7, 8).

Our solution of the three-dimensional structure of AChE from *Torpedo californica* (9) revealed that AChE indeed contains a catalytic triad similar to that present in other serine hydrolases (10). Unexpectedly, however, the active site of this unusually rapid enzyme is located at the bottom of a deep and narrow gorge, named the 'aromatic gorge', since it is lined primarily with the rings of fourteen aromatic residues (9, 11). Furthermore, the so-called 'anionic' binding site for the quaternary moiety of ACh does not contain a number of negative charges, as was earlier postulated on the basis of the ionic strength dependence of catalytic activity (12). Modeling studies suggested that interaction of the quaternary group is primarily with the indole ring of the conserved W84, and this was borne out by crystallographic studies on several AChE-ligand complexes, which also suggested a prominent role for F330 (13). This implication of aromatic residues as playing a prominent role in recognition of the quaternary group suggested by the X-ray studies was in agreement with parallel affinity and photoaffinity labeling studies carried out in solution (13, 14).

The availability of the three-dimensional structure of *Torpedo* AChE stimulated a large body of work, from a number of different laboratories, which shared the common objective of correlating the unexpected structure revealed by X-ray crystallography with the catalytic function of the enzyme. The studies carried out in this context can be loosely classed in four main categories, two theoretical and two experimental (obviously some studies encompass more than one of these categories):

1. Theoretical studies in which the structure of AChE or BChE from various sources is modeled on the basis of the 3-D structure of *Torpedo* AChE, taken together with the amino acid sequence of the cholinesterase in question, obtained previously from cloning and/or sequencing studies. A necessary condition for such modeling is the high sequence identity and similarity (ca. 50 % and 70 %, respectively) between cholinesterases of widely different phylogenetic origin (15, 16).
2. Theoretical studies aimed at elucidating the electrostatic and dynamic properties of the cholinesterase molecule, with the long-term objective of understanding their contribution to the known catalytic properties.
3. Experimental investigations concerned with the understanding the catalytic and ligand-binding properties of the cholinesterases on the basis of kinetic and spectroscopic studies utilizing AChE and BChE, both from *Torpedo* and from other sources.
4. Studies utilizing site-directed mutagenesis to understand the contribution of particular amino acid residues to the catalytic activity, substrate specificity and mode of interaction with reversible and covalent inhibitors of the various cholinesterase.

Obviously, in the context of this Midterm Report, it would be impossible to review in detail the multiple publications which have appeared in the 3 years since the 3-D structure of the *Torpedo* enzyme became known and was subsequently published (9). We will, nevertheless, try to deal with some of the main lines of research and principal conclusions reached.

Inspection of the 3-D structure of *Torpedo* AChE and of various AChE-ligand complexes, as well as of the structure of homologous enzymes, principally human AChE and BChE, inferred from modeling studies based on the 3-D structure of *Torpedo* AChE, led immediately to predictions about the involvement of certain amino acid residues, almost all localized in the 'aromatic gorge,' in various aspects of the enzyme's catalytic activity. Site-directed mutagenesis served as the principle tool for testing such predictions. Thus it was suggested, on the basis of the topology of the gorge (9), on the basis of X-ray structure of complexes of *Torpedo* AChE with the bisquaternary inhibitors decamethonium (13) and BW284c51 (Harel *et al.*, unpublished) and on the modeling of human BChE (16), that the so called 'peripheral' anionic site, previously identified on the basis of kinetic (17) and spectroscopic (18, 19) studies, was located at the top of the gorge and, like the 'anionic' subsite of the active site, contained three aromatic residues, namely Y70,

Y121 and W279 (*Torpedo* numbering is used here and subsequently). Kinetic comparison with BChE, which lacks all three of these residues, and with chicken AChE, which lacks two of them, provided strong experimental evidence to support this prediction (16, 20-23), and a role for the acidic residue, D72, in the 'peripheral' site was proposed, in addition, on the basis of site-directed mutagenesis data of this residue (24). Modeling also suggested a role for two aromatic residues, F288 and F290, in conferring narrow substrate specificity upon AChE as compared to BChE (25, 26), and this suggestion, too, was clearly borne out by mutagenesis studies.

Studies carried out to date have involved close to 200 mutations, carried out on human, mouse, *Torpedo* and *Drosophila* AChE, as well as human BChE (27). An updated compilation of these mutations can be obtained by accessing the Cholinesterase Data Base, at Montpellier, France, maintained by Arnaud Chatonnet. It is worth emphasizing that these mutagenesis studies leave numerous questions open. Thus, the data acquired so far ascribe specific roles to only seven of the conserved aromatic residues in the gorge, and the necessity for the remainder remains to be clarified. Furthermore, the role of two acidic residues, E199 and D72, respectively near the bottom and close to the top of the gorge, remains to be clearly ascertained. The long-standing question of the molecular basis for substrate inhibition also remains open. The possibility that it involves binding of a second ACh molecule at the 'peripheral' site, although attractive (20), is cast in doubt by mutagenesis studies (21, 28), by the observation that substrate inhibition is not very different for the chicken and *Torpedo* enzymes (23), and since mutation of E199, adjacent to the active site, can strongly reduce substrate inhibition (29). A complication which necessitates caution in analyzing all the site-directed mutagenesis is that in certain cases, mutations made at the top of the gorge appear to affect parameters ascribed to structural factors associated with the bottom of the gorge, and vice versa (24). Thus, the gorge may function in an integrated fashion which remains to be elucidated.

### III) RESULTS

#### A) *Acetylcholinesterase from Torpedo californica*

##### 1) Native enzyme and non-covalently bound inhibitor complexes

One of our principal objectives during the present stage of the project was to obtain higher resolution structures of the *Torpedo* enzyme, relative to the 2.8 Å structure (1ACE) obtained originally, published and deposited in the Brookhaven Protein Data Bank (PDB). To this end we have been carrying out data collection at two synchrotron facilities, using the DESY-EMBL beam line at Hamburg, and the X12c beam line of the NSLS at BNL. Using trigonal crystals obtained from PEG200, which are similar or identical in their characteristics to the trigonal crystals obtained previously from ammonium sulfate-phosphate buffer (9), we were able, at both facilities, to obtain data sets which diffracted out to 2.3 Å and had data of sufficiently high quality for meaningful refinement to 2.5-2.6 Å. A diffraction pattern showing spots out to 2.3 Å is shown in Fig. 1A, and a precession photograph for the same data is shown in Fig. 1B. We were also been able to obtain data sets for ligand-AChE complexes to similar resolution at both facilities, and this should greatly improve interpretation of the electron density maps for these complexes. Specifically, data were collected for complexes *d*-tubocurarine and huperzine A and EMBL-DESY, Hamburg and for edrophonium (EDR) at the NSLS at BNL. A data set for huperzine A showed diffraction out to 2.2 Å, and was refined to 2.5 Å resolution. This data set is in the process of being refined. The data set for *d*-tubocurarine diffracted out to only 2.9 Å, and was refined to this same resolution. It appears that the *d*-tubocurarine did not enter the crystal. This is most likely as the space that it is expected to occupy is, in fact, occupied by a symmetry-related molecule in the trigonal crystal structure (11). In order to obtain structures of complexes of peripheral site ligands with AChE it will be necessary to cocrystallization the ligand with the native enzyme. The data for the EDR-AChE complex, which were collected at BNL, yielded diffraction out to 2.2 Å, and the structure was refined to 2.5 Å resolution. The structure obtained for the EDR-AChE complex was virtually identical to that already reported in our previous final report under contract No. DAMD17-89-C-9063, now available from the PDB (IDCODE-1ACK), and subsequently published (13).

We have initiated a search for additional crystallization conditions, which might yield crystals diffracting to even higher resolution, or a crystal form in which the entrance to the active-site gorge would not be blocked by a symmetry-related molecule (11), as appears to be the case for both the trigonal and orthorhombic crystals obtained and studied so far. For this purpose, the AChE dimer preparation routinely employed (9, 30, 31) was further purified by gel filtration on Sephacryl

S300. The peak fractions were pooled, concentrated to ca. 12 mg/ml, and dialyzed against 0.05 M HEPES, pH 7.5.

Crystallization attempts using the hanging-drop procedure, in 36-40% PEG200/0.2 M MES, pH 5.6, yielded clusters of thin plate-like crystals. At ca. pH 8.0, above the isoelectric point of the enzyme, small crystals were obtained using both lithium sulfate and ammonium sulfate. The plate-like crystals obtained from PEG200 were characterized on the X12c beam line. The crystals were flash frozen in a stream of nitrogen at 98 K, so as to prolong their effective lifetime. Diffraction out to 2.3 Å was observed. Indexing and integrating, using the DENZO program, gave refined cell parameters  $a = 92.35$ ,  $b = 106.86$  and  $c = 150.95$  Å, in an orthorhombic space group,  $P2_12_12_1$ . The crystals displayed substantial mosaicity, possibly due to imperfect freezing conditions. It is worth noting that these orthorhombic crystals differ in both cell parameters and space group from the orthorhombic crystals which we obtained earlier from PEG200 (31).

A long-term objective of this project is to utilize state-of-the-art techniques of X-ray crystallography to carry out time-resolved studies. Use of the Laue technique, which utilizes polychromatic X-irradiation, enables data collection on a millisecond time scale. The group of Robert Sweet, at BNL, is carrying out such studies on the serine protease, trypsin, as well as on other proteins, on the X26c beam line (32, 33). In collaboration with them, we have already been able to obtain a Laue diffraction pattern for an orthorhombic crystal of *Torpedo* AChE diffracting out to 2.8 Å (Fig. 2), and we feel confident that it will be possible to obtain higher resolution with trigonal crystals.

## 2) Transition-state analog-AChE complex

Solution of the crystal structure of a complex of an enzyme with a powerful transition-state analog should greatly assist one's understanding of the principal interactions governing interaction of enzyme and substrate in the transition state. In the case of a rapid enzyme, such as AChE, it may be hoped that this, in turn, will help us to understand some of the factors underlying its remarkable catalytic power. Quinn and coworkers (34, 35) have studied the transition-state analog inhibitor, *m*-(*N,N,N*-trimethylammonio)trifluoroacetophenone (TMTFA) (36), in depth, and have shown that its  $K_i$  for inhibition of *Torpedo* AChE is 15 fM, i.e., that it binds about ten orders of magnitude more tightly than the substrate, ACh, in the ES complex. It seemed, therefore, to be a ligand of choice for achieving the above-mentioned objective. A complex of this ligand with *Torpedo* AChE was obtained by the same soaking methodology employed previously (13), incubating trigonal crystals in ammonium sulfate-phosphate buffer mother liquor, containing 2 mM

TMTFA, for 12 days at 19°C. Data collection was performed using a Rigaku rotating anode together with a Siemens-Xentronics area detector. Data were collected to 2.8 Å resolution. The structure was determined by the difference Fourier technique, and refined using simulated annealing and restrained refinement (37).

The overall conformations of native AChE and of the AChE-TMTFA complex are very similar, with rms = 0.4 Å for the C $\alpha$  atoms. The highest positive peak (7  $\sigma$ ) in the difference Fourier map was at bonding distance from S200O $\gamma$ , and its shape could accommodate a TMTFA molecule (Fig. 3). A model of TMTFA was generated using the coordinates of EDR (13) to build the (trimethylammonium)phenyl moiety, and those of ACh to construct the trifluoroaceto moiety, adjusting the C-F distance to be 1.5 Å. The final refinement parameters which were thus obtained were:

R factor = 0.188

R<sub>free</sub> = 0.235

Water molecules = 99

Sulfate molecules = 1

rms bond = 0.007 Å

rms angle = 1.016°

The TMTFA molecule occupies the positions of six water molecules (in the 2.25 Å native structure). Upon binding to TMTFA, S200O $\gamma$  swings from its position in the native structure to become a partner in a tetrahedral conformation around the aceto C, at a distance of 1.4 Å from it (Fig. 4). The sulfate ion is located further up the active-site gorge, displacing three water molecules in the native structure; it makes a single H-bond to F288N.

Close inspection of the structure of the TMTFA-AChE structure, as displayed in Fig. 4, reveals that the ligand in this complex is oriented very similarly both to EDR in the EDR-AChE complex already published (13), and to ACh in the model obtained by docking the ACh molecule in an all-*trans* conformation into the crystal structure of the *Torpedo* enzyme (9). As already indicated, the carbonyl carbon of the trifluoroketone function interacts covalently with O $\gamma$  of the S200-E327-H440 catalytic triad. As predicted (9), there appears to be tripartite hydrogen-bonding between the incipient oxyanion and the NH functions of G118, G119 and A201, and substantial interactions of the quaternary group with the aromatic rings of W84 and F330, as well as with that of Y130 and with the carboxyl function of E199. The trifluoromethyl function fits very well into the acyl-binding pocket which is provided principally by the phenyl groups of F288 and F290.



These multiple interactions, taken together, help to explain the remarkable catalytic power of AChE. Since, in fact, they envelop the ligand from all sides, it seems plausible that burying the active site at the bottom of the aromatic gorge may be a prerequisite for obtaining a highly effective transition state.

### 3) Organophosphoryl-AChE conjugates

We are using, as an initial stage in our structural work on OP-AChE conjugates, the same pair of conjugates as we used in our study comparing 'aged' and 'non-aged' OP conjugates of chymotrypsin (38). Thus, into crystals of *Torpedo* AChE, we are soaking paraoxon to obtain diethylphosphoryl-AChE (DEP-AChE), a representative 'non-aged' OP conjugate, and diisopropyl fluorophosphate (DFP) to obtain monoisopropyl-AChE (MIP-AChE), a representative 'aged' conjugate. The success of this approach has been already demonstrated by our obtaining a partially complete (*ca.* 70 %) data set for DEP-AChE, using an orthorhombic crystal. Although the incompleteness, due to a technical failure, rendered this data set unsatisfactory for achieving our objective of visualizing a high resolution structure of the conjugate, it was adequate to demonstrate that the paraoxon had penetrated the crystal and reacted to form the conjugate. It is possible that paraoxon may not have full occupancy in the AChE crystals. If so, longer soaking times may be required, as was the case for chymotrypsin, where several weeks of soaking were found to be necessary (38). It is also clear that better data, at higher resolution, will have to be collected in order to see the possible subtle changes in the AChE structure upon interaction with paraoxon as was required in our studies with chymotrypsin (38). We are currently carrying out structural studies utilizing conjugates obtained employing trigonal crystals, and hope to have better structural data in the future.

### ***B) Human Recombinant AChE***

In our attempts to obtain crystals of human AChE we have been exploring use of human recombinant AChE (HrAChE) from two sources. In both cases, the human AChE clone of Soreq and coworkers (39) was expressed. Thus, we have been attempting to characterize and crystallize HrAChE expressed in eukaryotic and prokaryotic expression systems, namely, in the human kidney 293 cell line, by Avigdor Shafferman, Baruch Velan and coworkers at IIBR (40, 41), and in *Escherichia coli* by Meir Fischer and coworkers at Biotechnology General (42). Both groups have generously provided material for this purpose.

### 1) HrAChE expressed in *Escherichia coli*

This material was obtained in purified form from Biotechnology General, purification having been carried out as described (42). Prior to screening of crystallization conditions, it was dialyzed against 0.25 M NaCl/0.01 M Tris, pH 8.0, containing 1 mM each of phenylmethylsulfonyl fluoride, dithiothreitol and benzamidine, passed over a Sephacryl S300 column equilibrated with the same buffer, dialyzed against the same buffer as before, but containing only 10 mM NaCl, and concentrated to *ca.* 10 mg/ml. Microcrystals were obtained under a few conditions, but none of size worth pursuing further at this stage.

It was noted that, although this preparation was rather pure as judged by SDS-PAGE and on the basis of its specific activity, it contained a mixture of species, corresponding to monomer, dimer and tetramer, as analyzed by sucrose gradient centrifugation. The ratio of these forms could be modified by changing the pH and/or the ionic strength, or by adding a small amount of neutral detergent. Although it was difficult to determine reproducible conditions for obtaining a monodisperse preparation, this heterogeneity may have been the reason why our crystallization attempts had limited success. It has, however, been suggested that the presence of low concentrations of a neutral detergent may be beneficial for such a system (A. McPherson, personal communication), and we intend to explore this possibility.

### 2) HrAChE expressed in 293 cells

In our attempts to crystallize HrAChE expressed in human kidney cells, we have been obtaining large amounts of culture medium from Dr. Avigdor Shafferman and his coworkers, at IIBR, from which we have then been purifying the AChE to be used for crystallization attempts, employing an affinity chromatography procedure similar to that developed for purification of the *Torpedo* enzyme (30, 31). Two problems to be overcome in this context are heterogeneity of molecular forms of AChE (41) and the presence of protease activity in the culture medium (A. Shafferman, personal communication). To deal with the proteases, we have routinely been eluting the AChE from the affinity column with an elution buffer containing an anti-protease cocktail (43). So as to overcome the problem of heterogeneity, Dr. Shafferman has been supplying us with culture medium enriched in either tetramers (medium obtained with younger cultures) or monomers (from older cultures), dimers usually accounting for a minor percentage of the total activity in either case. Since neither the older or younger cultures contain exclusively one form or the other, we

then attempt to obtain a homogeneous preparation by passing the affinity-purified AChE, subsequent to concentration to a small volume, over a Sephacryl S300 column. Starting from 2 liters of culture medium, it has been possible to obtain batches of 10-20 mg of highly purified HrAChE, as judged by SDS-PAGE. Fig. 5 shows the sucrose-gradient centrifugation pattern of a purified sample containing principally monomer (*ca.* 5 S), but also a substantial amount of tetramer (*ca.* 10 S). Passage of this preparation over a Sephacryl S300 column also yielded two peaks, the smaller peak eluting first (Fig. 6). Sucrose gradient centrifugation of the smaller peak revealed a major 10 S component, totally devoid of more slowly sedimenting species (Fig. 7A), while similar analysis of the major peak revealed a major component sedimenting at 5 S, with a minor 6 S component also present, but very little heavier material (Fig. 7B). SDS-PAGE revealed that both peaks consisted of highly purified enzyme (Fig. 8). Although attempts to crystallize the pool from the S300 column which corresponds to tetramer have met with little success so far, we have obtained microcrystals from the monomer pool in a number of cases. Fig. 9 shows crystals obtained at 4°C from 0.2 M ammonium acetate/0.1 M sodium citrate, pH 3.6, containing 30% 2-methyl-2,4-pentanediol.

### C) *Bungarus fasciatus* AChE

In collaboration with Cassian Bon (Unité des Venins, Institut Pasteur, Paris) and Jacques Grassi (CEA, Saclay), who are supplying us with preparations of highly purified enzyme, we are attempting to obtain crystals of the monomeric form of AChE present in large amounts in the venom of the krait, *Bungarus fasciatus*. This task was approved as a no-cost modification of the SOW. The purified *Bungarus* AChE obtained from our French colleagues was passed over a Sephacryl S300 column so as to remove trace impurities and insoluble material, dialyzed against 0.01 M NaCl/0.01 M Tris, pH 8.0, and concentrated to *ca.* 10 mg/ml. Preliminary screening revealed a number of conditions in which small crystals could be obtained. These included 0.4-0.5 M ammonium phosphate, pH 7.5, and ammonium sulfate at various pH values. Measurements on the NSLS beam line, X12c, at BNL, on crystals of dimensions 0.02x0.02x0.015 mm, at 90 K, showed diffraction out to 3.5 Å resolution (Fig. 10).

As a byproduct of this project we have taken advantage of the monomeric character of the snake venom enzyme so as to measure its dipole moment directly, this being done in collaboration with Dietmar Pörschke (Max-Planck-Institut für Biophysikalische Chemie, Göttingen), who is an expert in performing electrooptical measurements. He has been able to show that the *Bungarus*

*fasciatus* monomer does, indeed, possess a large permanent dipole moment (*ca.* 1000 Debye), of the same order as that calculated for the *Torpedo* enzyme (44). Since cloning experiments, in Dr. Bon's laboratory, are at an advanced stage, it will soon be possible to calculate the dipole moment of the snake venom enzyme by use of a model of its 3-D structure generated from the 3-D structure of the *Torpedo* enzyme, so as to see whether the theoretical calculations are in agreement with the value measured experimentally.

#### **D) Horse Serum BChE**

In collaboration with Dr. B.P. Doctor (Walter Reed Army Institute of Research) we are attempting to obtain crystals of horse serum BChE purified in his laboratory. This task, too, was approved as a no-cost modification of the SOW. In a preliminary screening crystals, were obtained from 0.2 M ammonium phosphate/0.1 M Tris, pH 8.5, containing 50% 2-methyl-2,4-pentanediol (Fig. 11). These crystals, although still small, seem very promising candidates for structural studies. Apart from permitting a detailed comparison of the active sites of AChE and BChE, solution of their structure will also allow us to see the arrangement of subunits in a cholinesterase tetramer. Measurements on the NSLS beam line, X12c, at BNL, did not reveal any protein diffraction pattern, but they did not reveal a salt diffraction pattern either, excluding the possibility that the crystals obtained were salt crystals.

#### **E) Theoretical Studies**

##### **1) Electrostatic properties of AChE**

In collaboration with Daniel Ripoll and Carlos Faerman (formerly at the Biotechnology Institute, National Research Council of Canada, Montreal, and currently at Cornell University, Ithaca) we have carried out electrostatic potential and field calculations based on the crystal structure of *Torpedo* AChE, employing for this purpose the program DELPHI (45, 46). These calculations reveal that AChE possesses a remarkably strong electric dipole, *ca.* 500 Debye (44). Contours of electrostatic potential reveal that the enzyme subunit possesses a negative isopotential extending over half the protein surface, and a positive isopotential extending over the other half (Fig. 12). The dipole is aligned with the aromatic gorge leading to the active site, and its direction is such that a positively charged species, e.g., the quaternary substrate, ACh, would be drawn into and down the gorge by the electrostatic field (Fig. 13). Within the gorge, the aromatic side chains appear to shield the substrate from direct interaction with most of the negatively charged residues

which give rise to the dipole. The affinity of quaternary ammonium groups for aromatic rings, coupled with this electrostatic force, may work in concert to create a selective and efficient binding site for AChE. Another enzyme, *Geotrichum candidum* lipase, which like AChE, is a member of the  $\alpha/\beta$  hydrolase fold family (47), and also displays considerable sequence homology with AChE (48), is totally devoid of the asymmetric charge distribution of AChE, which is not surprising in view of the fact that its substrate is a neutral molecule.

As mentioned above, in collaboration with Dietmar Pörschke (Max-Planck-Institut für Biophysikalische Chemie, Göttingen), electrooptical measurements, utilizing a monomeric form of AChE purified from *Bungarus fasciatus* venom, have provided direct experimental proof that AChE indeed possesses a large permanent dipole moment, *ca.* 1000 Debye.

## 2) Structure and dynamics of the active-site gorge

Close inspection of the 3-D structure of *Torpedo* AChE revealed that, in the crystal lattice, a symmetry-related subunit appears to block the mouth of the active-site gorge completely (11). This observation was particularly intriguing, since we had experienced no difficulty in soaking various quaternary ligands into the AChE crystals so as to obtain several ligand-AChE complexes (see, for example, (13)). Detailed inspection revealed that the gorge was 20 Å deep, with an irregular cross-section, and an average diameter of 4.4 Å. This compares to 6.4 Å for the van der Waals diameter of the quaternary group of ACh. Thus, ACh and other quaternary ligands are too large to enter and exit the active site through the gorge as visualized in the X-ray structure, even if it is not blocked by a symmetry-related molecule as observed in the crystal structure (see above). These two observations, taken together with the fact that the electric dipole attracting ACh into the gorge would retard the movement of choline out of the gorge (see Section III.E.1), prompted us to examine the structure and dynamics of the gorge more carefully, with a view to discovering additional sites for ingress and egress of substrates, products and water, as well as of other quaternary ligands (11).

Whereas roughly 3/4 of the walls of the aromatic gorge are 2 or more residues thick, 1/4 is relatively thin, i.e., only 1 residue thick (Fig. 14). This thin aspect of the gorge wall is comprised entirely of the sequence of residues between Cys67 and Cys94, which are disulfide-linked, thus comprising an  $\omega$  loop (49), and display little interaction with other parts of the protein. This is of particular interest, due to the structural homology of AChE with other members of the  $\alpha/\beta$  hydrolase fold family (47), including several neutral lipases (48). Such lipases contain a flap lying

over their active site (50), which may play an important role in their interfacial activation (51). This flap corresponds to the  $\omega$  loop just mentioned, which includes Trp84, with the indole ring of which the quaternary group of ACh is believed to interact (9, 13, 14). Simulated annealing runs, employing the program SYBYL, revealed that the Cys67-Cys94 can undergo substantial movement, especially W84. One way to test whether movement of this loop might be involved in the mechanism of AChE, by providing a 'back-door' or 'side door', would be to 'lock' it into the main body of the protein, by using site-directed mutagenesis to create a novel salt-bridge or disulfide bond. Modeling studies suggest that such a disulfide bond should form in the double mutant, G80C/V431C, and mutagenesis studies are being carried out in collaboration with the group of Jean Massoulié, at Ecole Normale Supérieure in Paris, to test this possibility.

In collaboration with an additional group of theoreticians at the University of Houston, headed by Andy McCammon and including Mike Gilson, a second 'back door' model was considered (52). Thus a molecular dynamics simulation, utilizing the program QUANTA, revealed transient opening (0.3 ps) of an aperture large enough to pass a water molecule. This transient opening was generated by simultaneous movement of Glu441, Trp84 and Val129, and might be described as a 'shutter' model for the putative 'back door'. Although the aperture was small and short-lived, it occurred within 20 ps of initiation of the molecular dynamics simulation. It is possible that such an aperture, if confirmed experimentally, might serve as a water vent, keeping in mind that movement of substrate down the narrow gorge might be expected to exert hydrostatic pressure on the water with which the gorge is filled (9, 11). Naturally, the question arises whether, over a longer time scale, the 'shutter' might open wider to permit transit of reaction products. It is of interest that comparison of the electrostatic properties of the AChE molecule modeled with this 'back door' open, as compared to the native AChE structure (1ACE), in which the 'back door' is closed, revealed a strong field at the 'back door' in the open configuration, whose direction would repel acetate from the active site, but would attract choline inwards. Thus this 'shutter' model, in its present form, does not provide a satisfactory model for traffic through the gorge. A test for the 'shutter' model was proposed, based on site-directed mutagenesis of Val129 to an Arg residue, which would form a putative salt bridge with Glu445. The mutation V129R, as well as a number of similar mutations, was carried out for *Torpedo* AChE in collaboration with the laboratory of Jean Massoulié, and no significant effect on the kinetic parameters was observed. Similar experiments, carried out for human AChE by the Shafferman group (53) were similarly negative. Although these negative experiments cannot rule out the 'shutter' model in its present form, they certainly cast serious doubt on its validity. It should be borne in mind that as the putative salt bridge formed by these mutations would be near or at the surface, it might be rather weak, and thus would not serve as a definitive test of the 'back door' hypothesis.

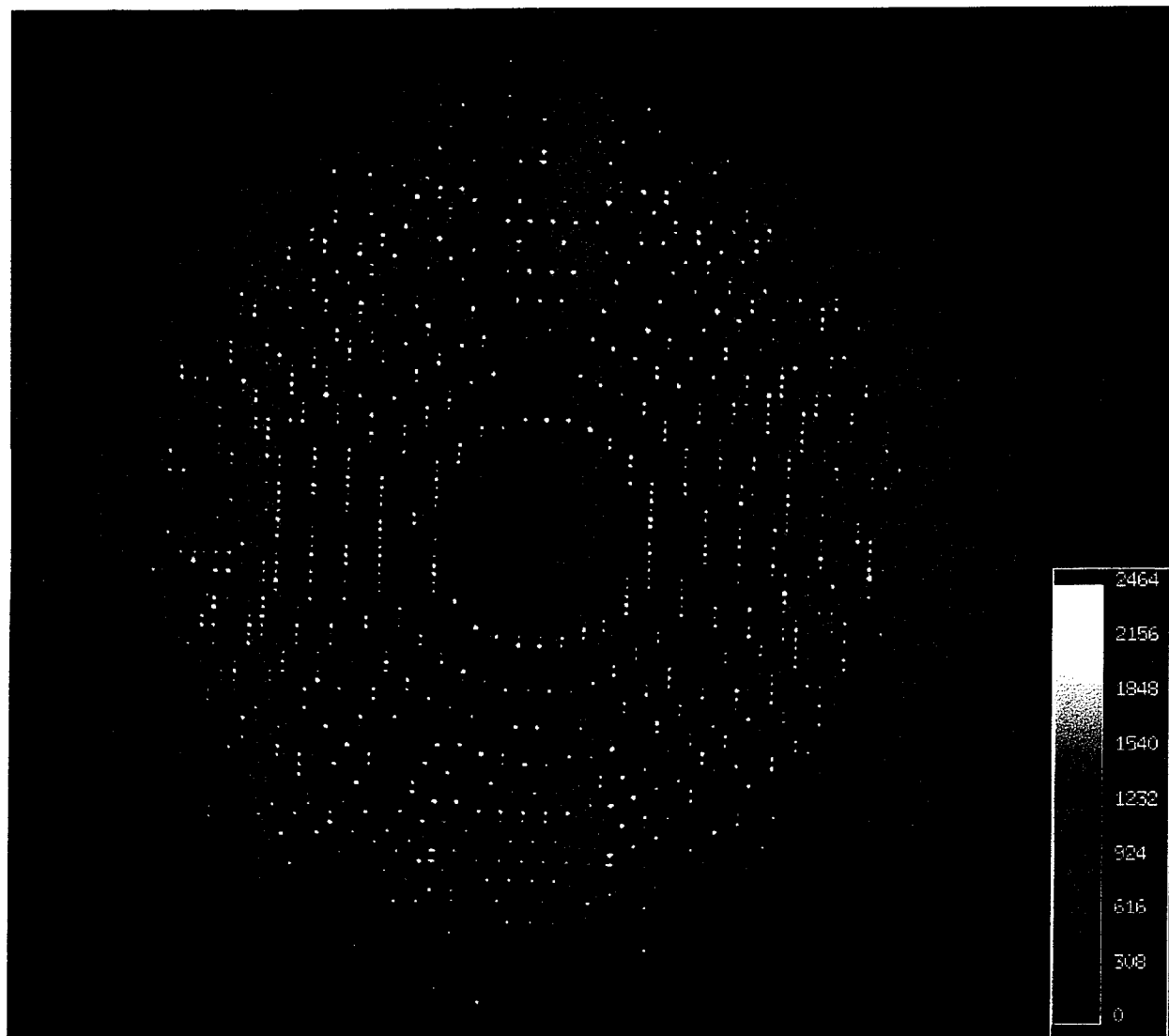


**Figure 1A.** Diffraction pattern of a native *T. californica* AChE crystal. The crystals were grown from PEG and show spots out to 2.3 Å. A 1° oscillation photograph, exposure time 180 seconds, at 90 K, collected at the BNL-NSLS beam line X12c.

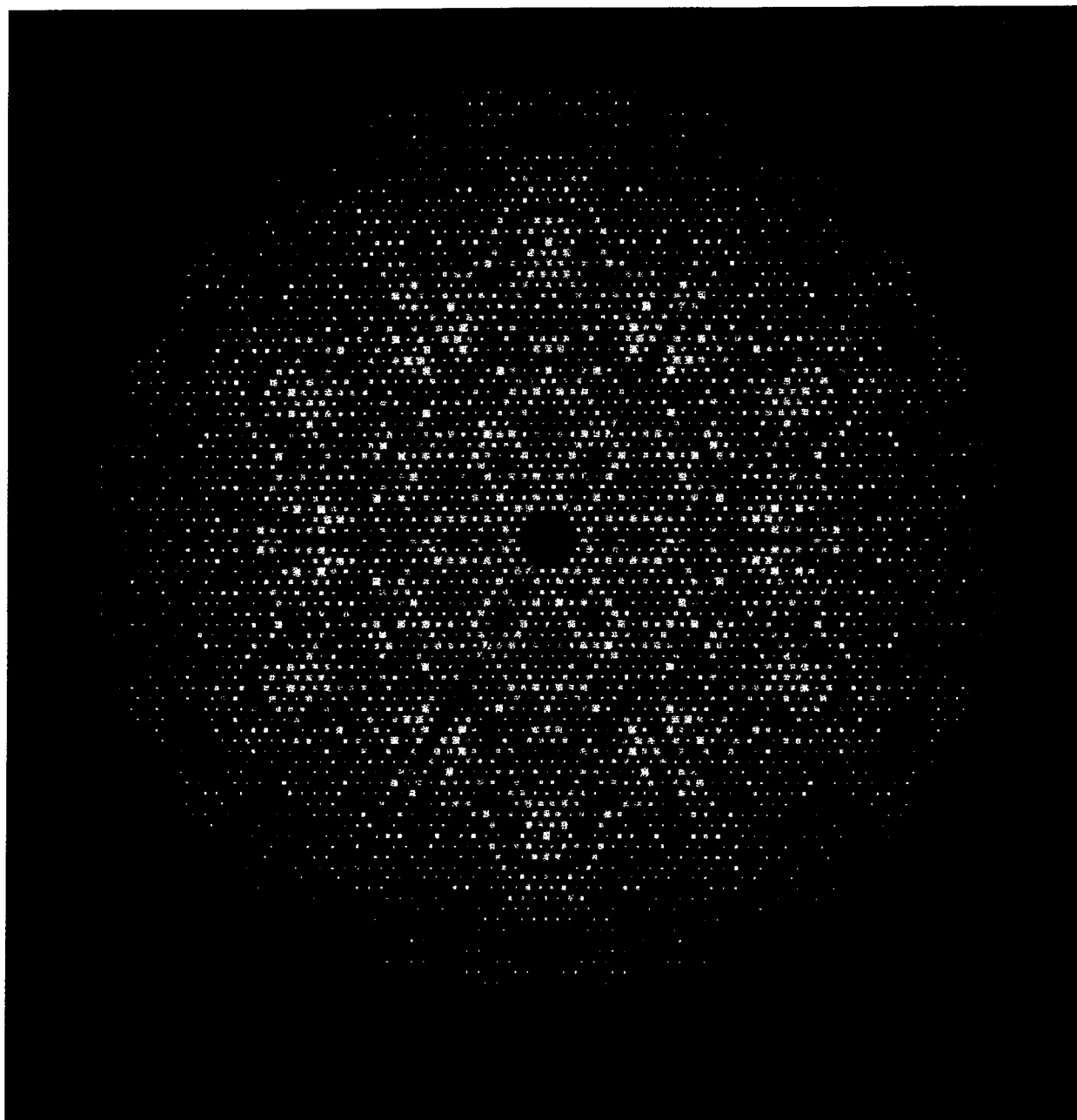


**Figure 1B.** Precession photograph of a native *T. californica* AChE crystal. The crystal is the same as in Fig. 1A, and the precession photograph generated is down the unique *c* axis and is based on the full set of oscillation photographs collected.



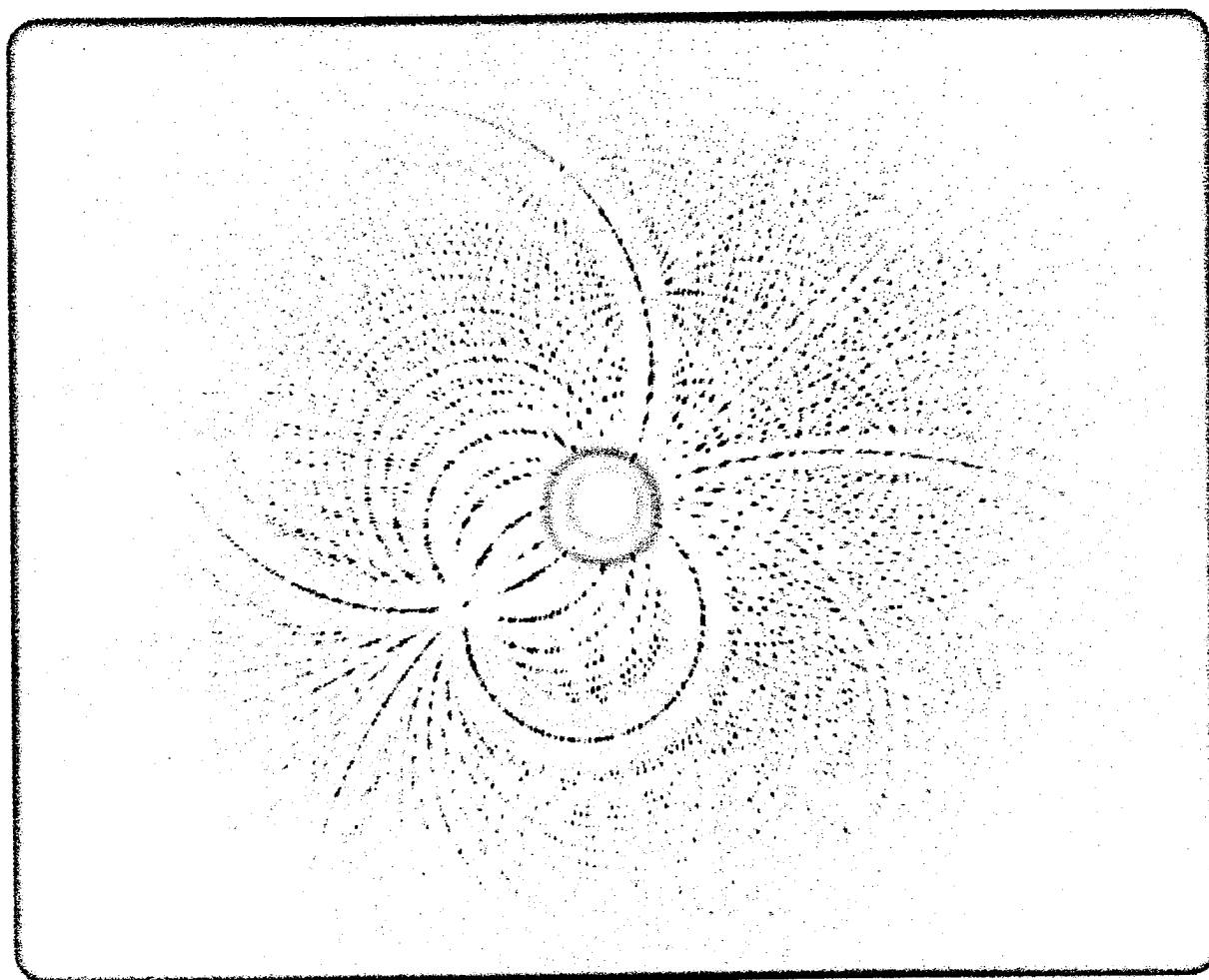
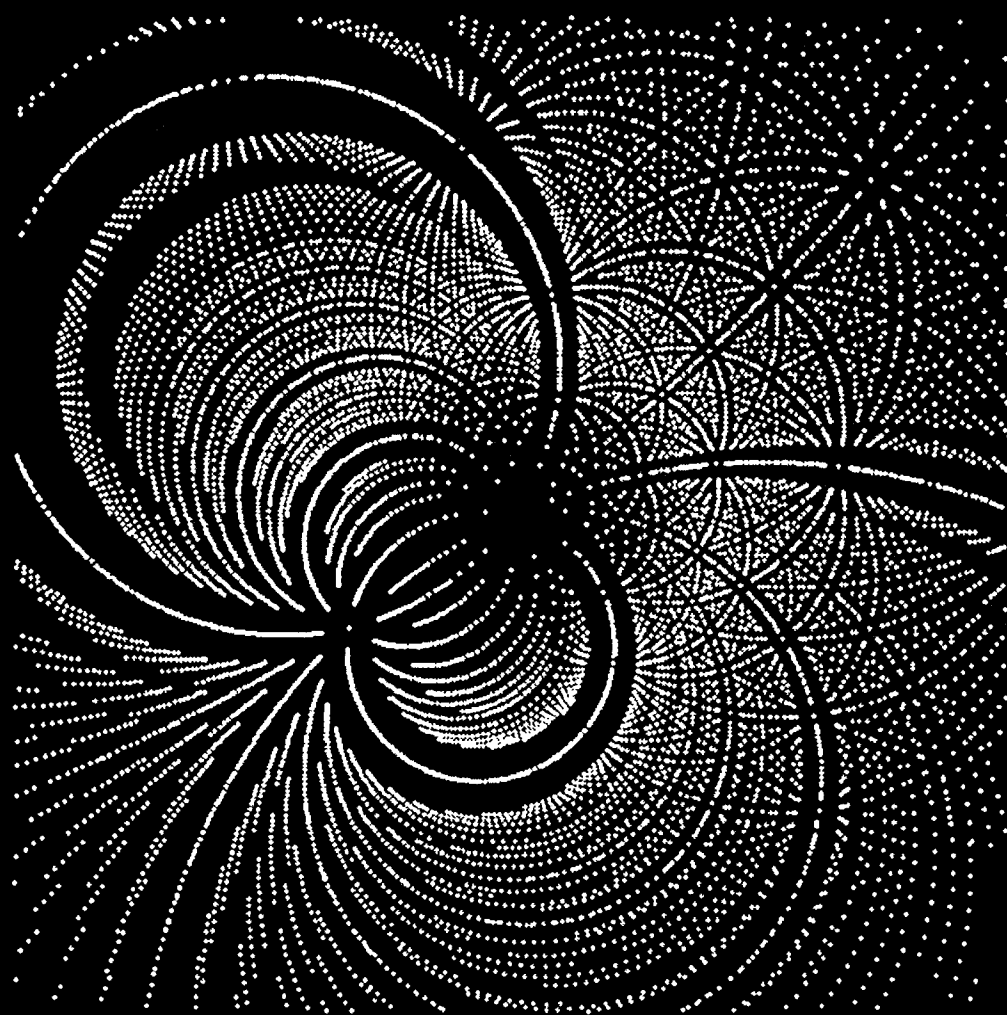


**Figure 2A.** Laue diffraction pattern for an orthorhombic crystal of *Torpedo* AChE. The crystal diffracted out to 2.8 Å. 6 msec exposure.

## Acetylcholinesterase



Exposure time: 6ms. NSLS X26C Aug '94

**Figure 2B.** Overlay of observed and simulated Laue diffraction patterns. The patterns are from the same crystal as shown in Fig. 2A.

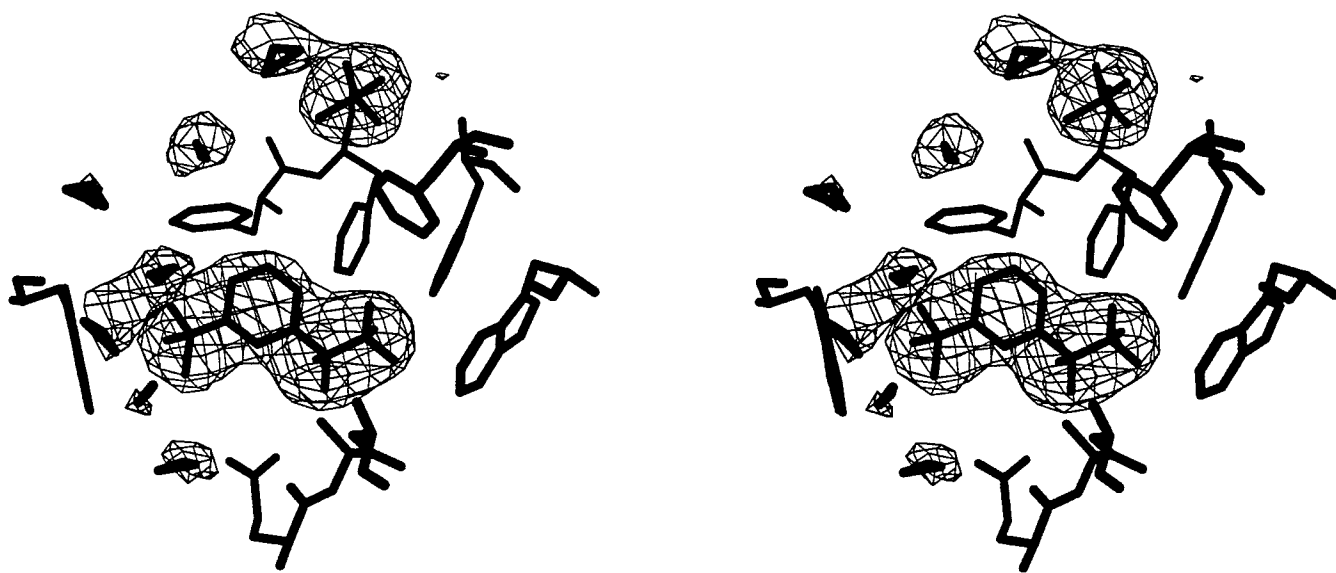
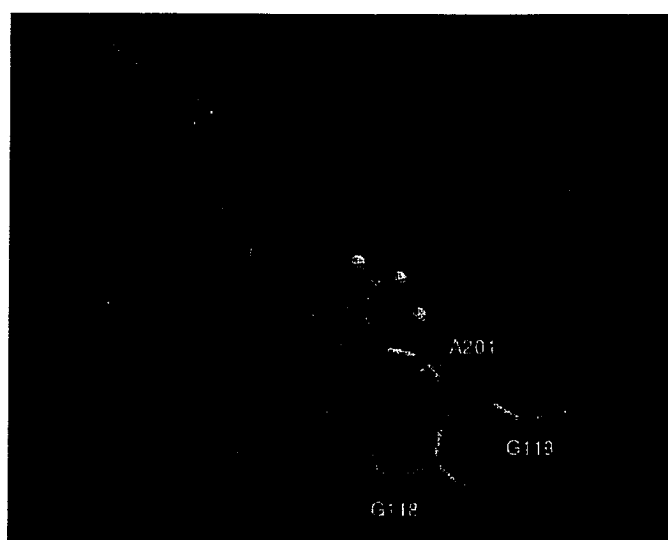
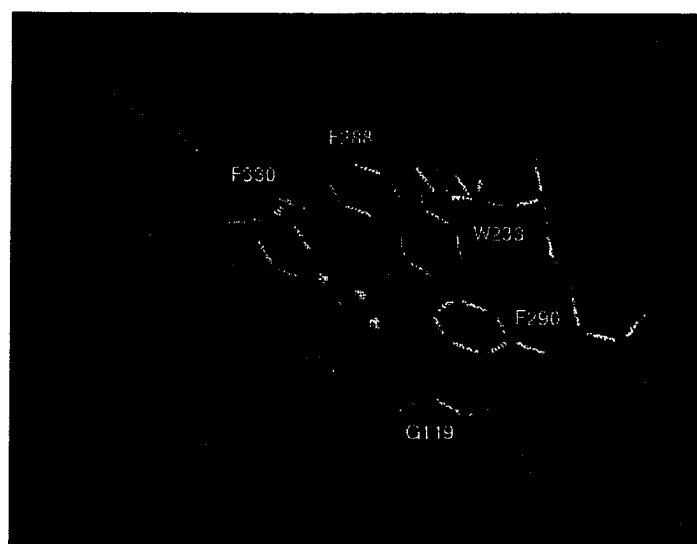


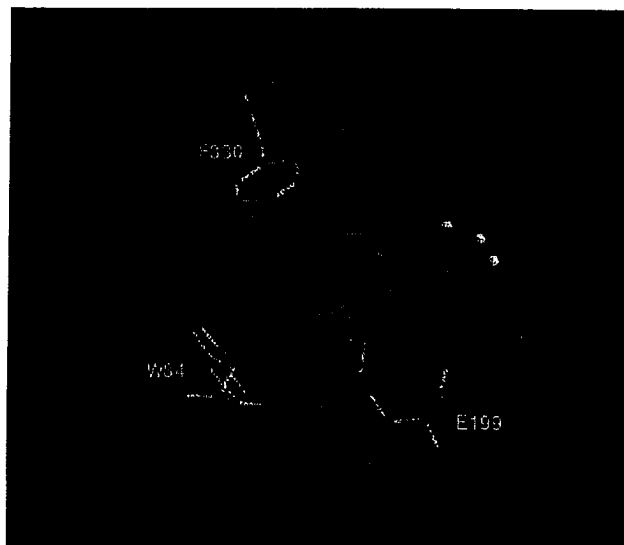
**Figure 3.** Stereo omit map of the refined structure of the TMTFA-AChE complex. The map is contoured at  $3\sigma$ . Electron density is seen for the covalently bound TMTFA, a sulfate ion (SUL) and 7 water molecules.



**A**



**B**



**C**

**Figure 4.** Hydrogen bonds and close distances between TMTFA and AChE. A) Catalytic triad and oxyanion hole interactions; B) Quaternary nitrogen group interactions; C) Trifluoroacyl interactions. TMTFA is shown in light blue, the catalytic triad in red, other AChE residues in orange and waters in purple.

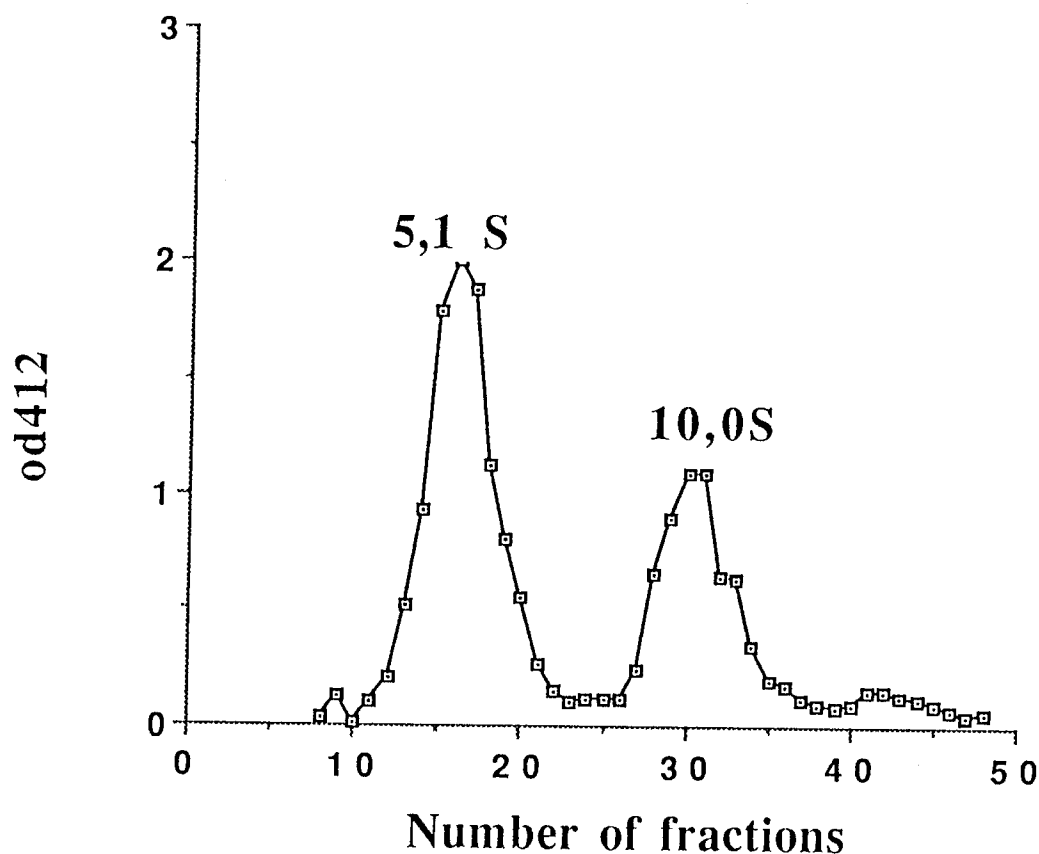


**Figure 5.** Sucrose gradient centrifugation of affinity-purified HrAChE. Centrifugation was performed on 5-20% sucrose gradients in 0.1 M NaCl/0.01 M Tris, pH 8.0, containing an antiprotease cocktail (10 mM EDTA - 10 mM EGTA - 1 mg/ml bacitracin - 40  $\mu$ g/ml leupeptin - 1 mg/ml aprotinin - 5 mM *N*-ethylmaleimide - 2 mM benzamidine). Centrifugation was for 18 h at 4°C using a SW40 rotor in a Beckmann L7-55 ultracentrifuge. Catalase (11.4 S) served as an internal marker.

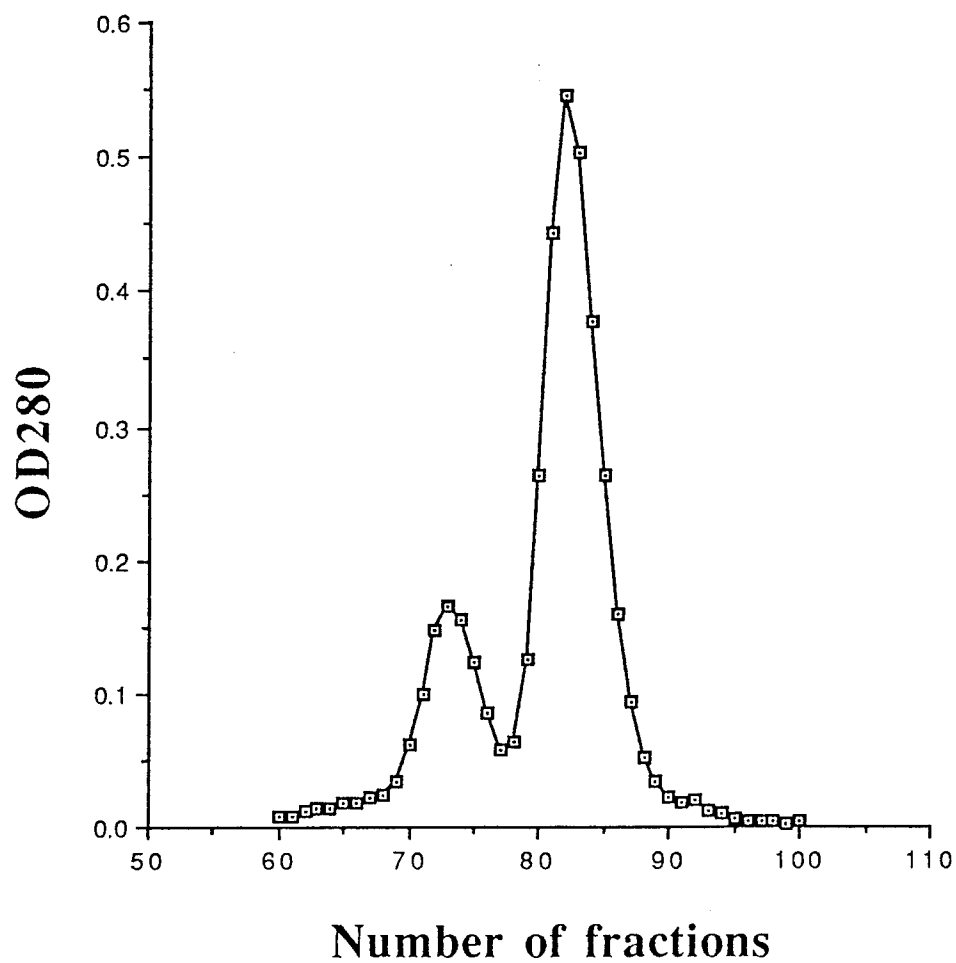


**Figure 6.** Gel filtration of affinity-purified HrAChE on a Sephacryl S-300 column. Gel filtration was performed in 0.25 mM NaCl/0.01M Tris, pH 8.0, containing 0.02% sodium azide, on a 2.6x100 cm column at 4°C.

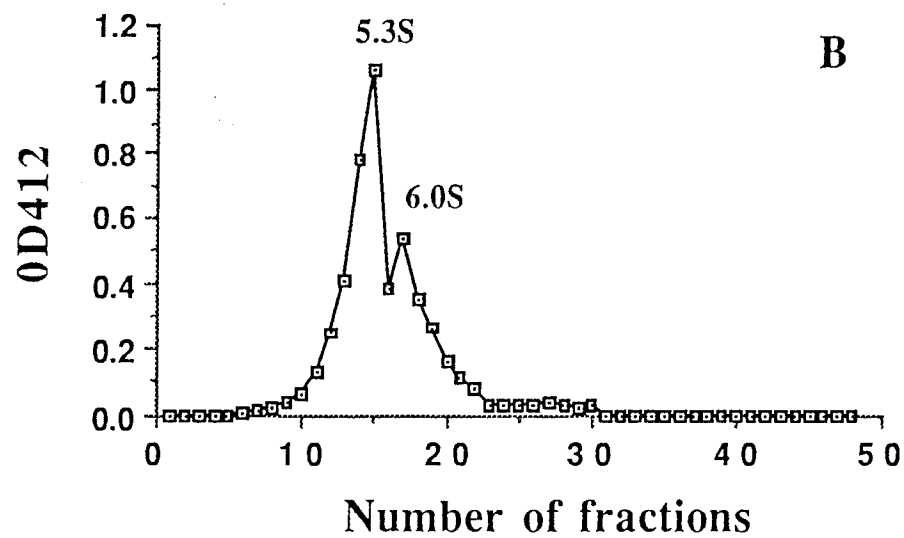
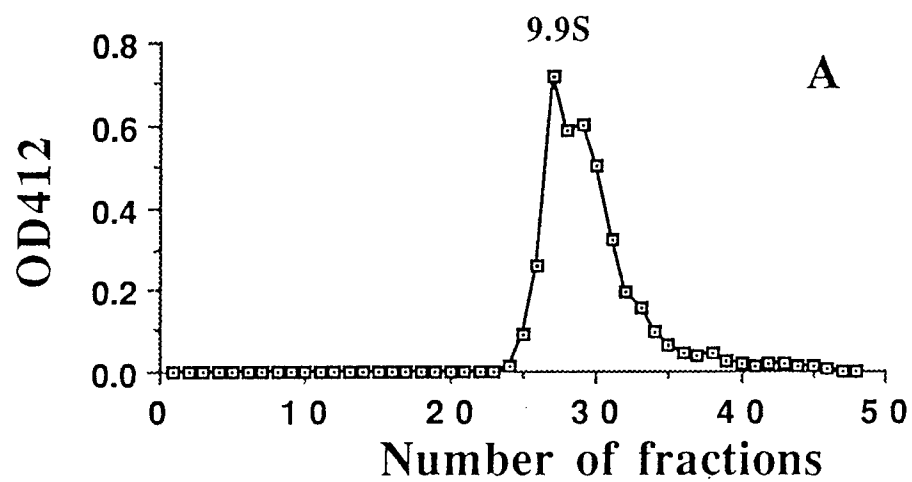


**Figure 7.** Sucrose gradient centrifugation of the peaks separated on the Sephacryl S-300 column. A) Minor peak; B) Major peak. Centrifugation was performed as described in the legend to Fig. 5, except that the antiprotease cocktail was omitted.

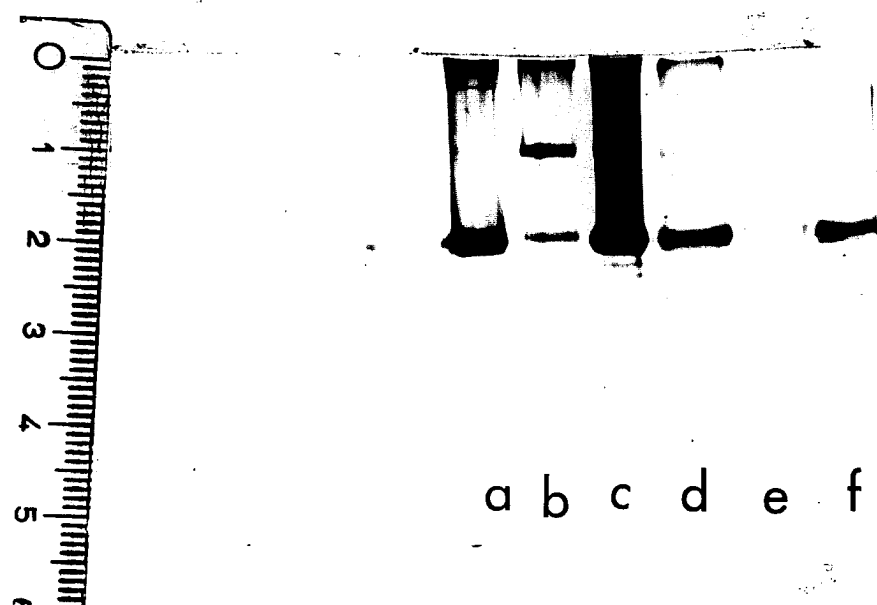


**Figure 8.** SDS-PAGE of affinity-purified HrAChE before and after gel filtration. Electrophoresis was performed under non-reducing (lanes a-c) and reducing (lanes d-f) conditions. a) Major peak (corresponding to  $G_1$  AChE); b) Minor peak (corresponding to  $G_4$  AChE); c) Material applied to the column; d) as in (a), but under reducing conditions; e) as in (b), but under reducing conditions; f) as in (c), but under reducing conditions. It can be seen that in the  $G_1$  peak, as expected, subunit monomers predominate even under non-reducing conditions (lane a), whereas in the  $G_4$  peak, subunit dimers predominate (lane b).





**Figure 9.** Crystals of monomeric HrAChE. The enzyme was expressed in 293 cells, and crystals were obtained from 0.2 M ammonium acetate/0.1 M sodium citrate, pH 3.6, containing 30% 2-methyl-2,4-pentanediol, at 4°C.

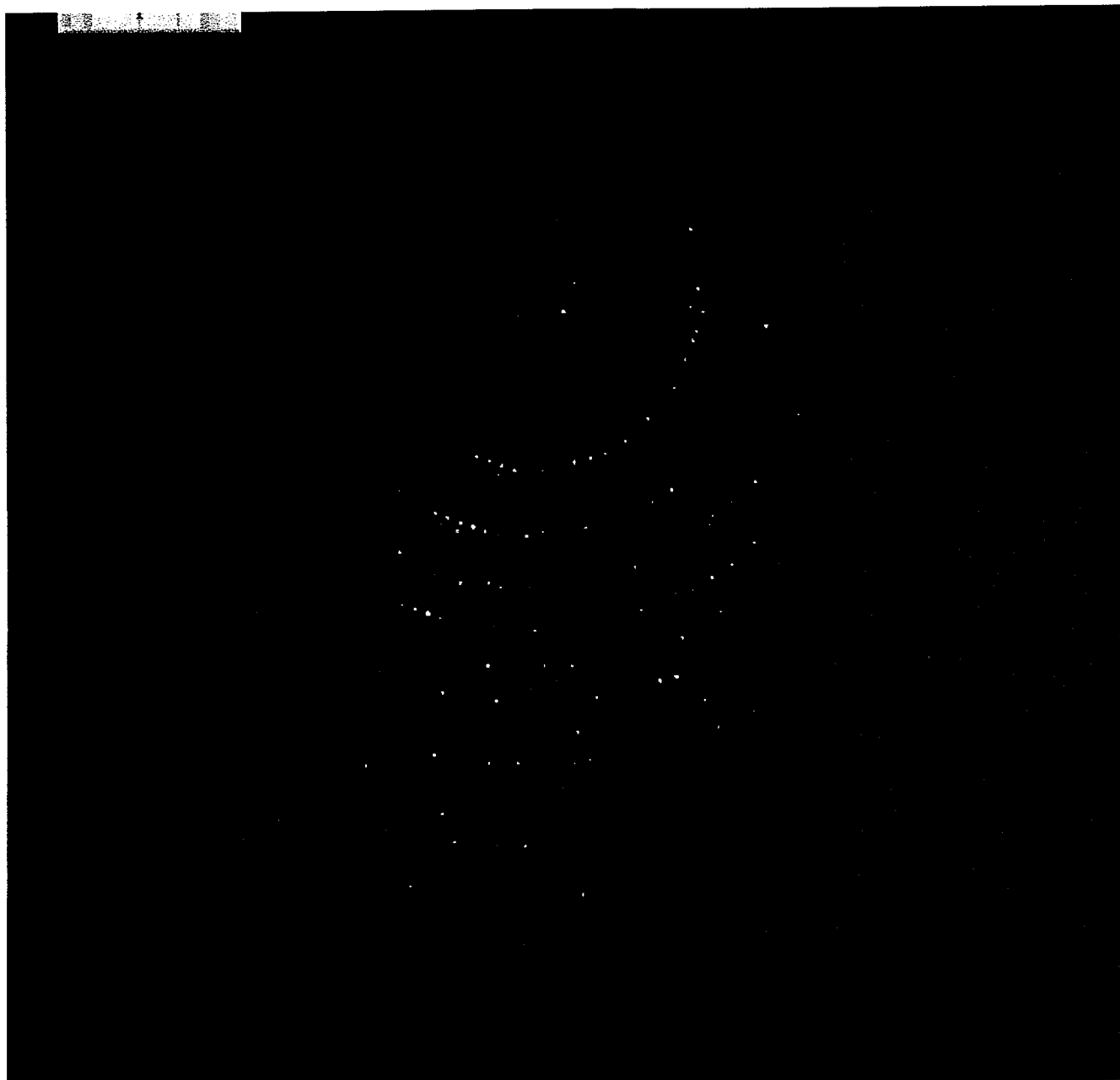


**Figure 10.** Diffraction pattern of *Bungarus fasciatus* AChE crystals. Crystals were grown from 0.3 M ammonium phosphate, pH 8.4, at 4°C. The diffraction pattern shows spots out to 3.5 Å. This is a 1° oscillation photograph, exposure time 300 seconds, at 90 K, collected at the BNL-NSLS beam line X12c.

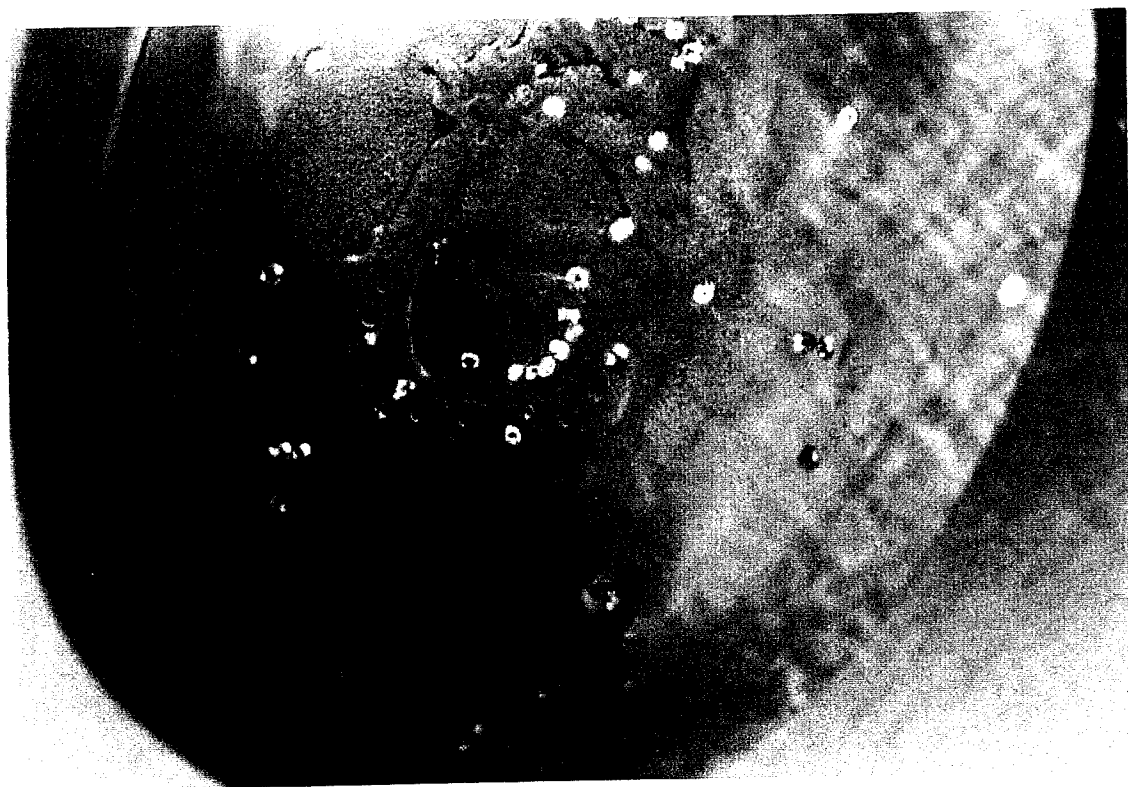


**Figure 11.** Crystals of horse serum BChE. The crystals were grown from 0.2 M ammonium phosphate/0.1 M Tris, pH 8.5, containing 50% 2-methyl-2,4-pentanediol, at 4°C.

## AcChoEase

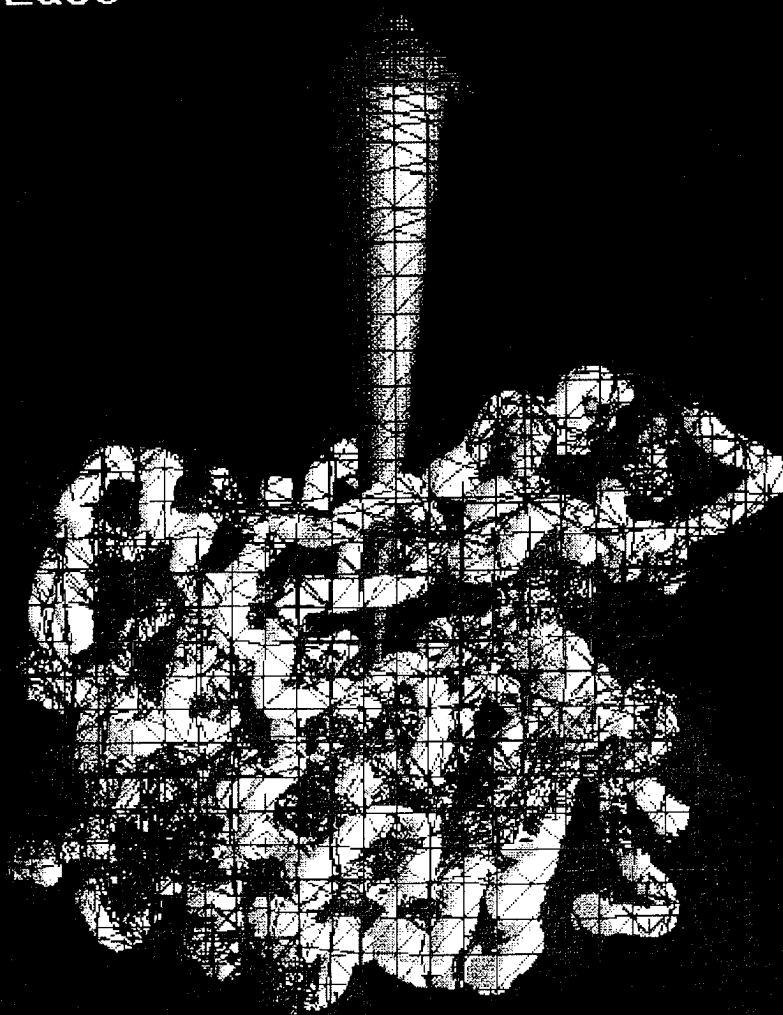


**Figure 12.** Backbone drawing of AChE with electrostatic isopotential surfaces superimposed. This figure was generated with the program GRASP (A. Nicholls and B. Honig, Columbia Univ., NY). Orientation of the protein is with the active-site gorge pointing upwards in the middle of the figure. The backbone of the protein is represented by white 'worms.' The red surface corresponds to the isopotential contour  $-1kT/e$ , and the blue surface to the isopotential contour  $+1kT/e$ , where  $k$  = the Boltzmann constant,  $T$  = temperature, and  $e$  = electronic charge. Arrow indicates the direction of the dipole in acetylcholinesterase.

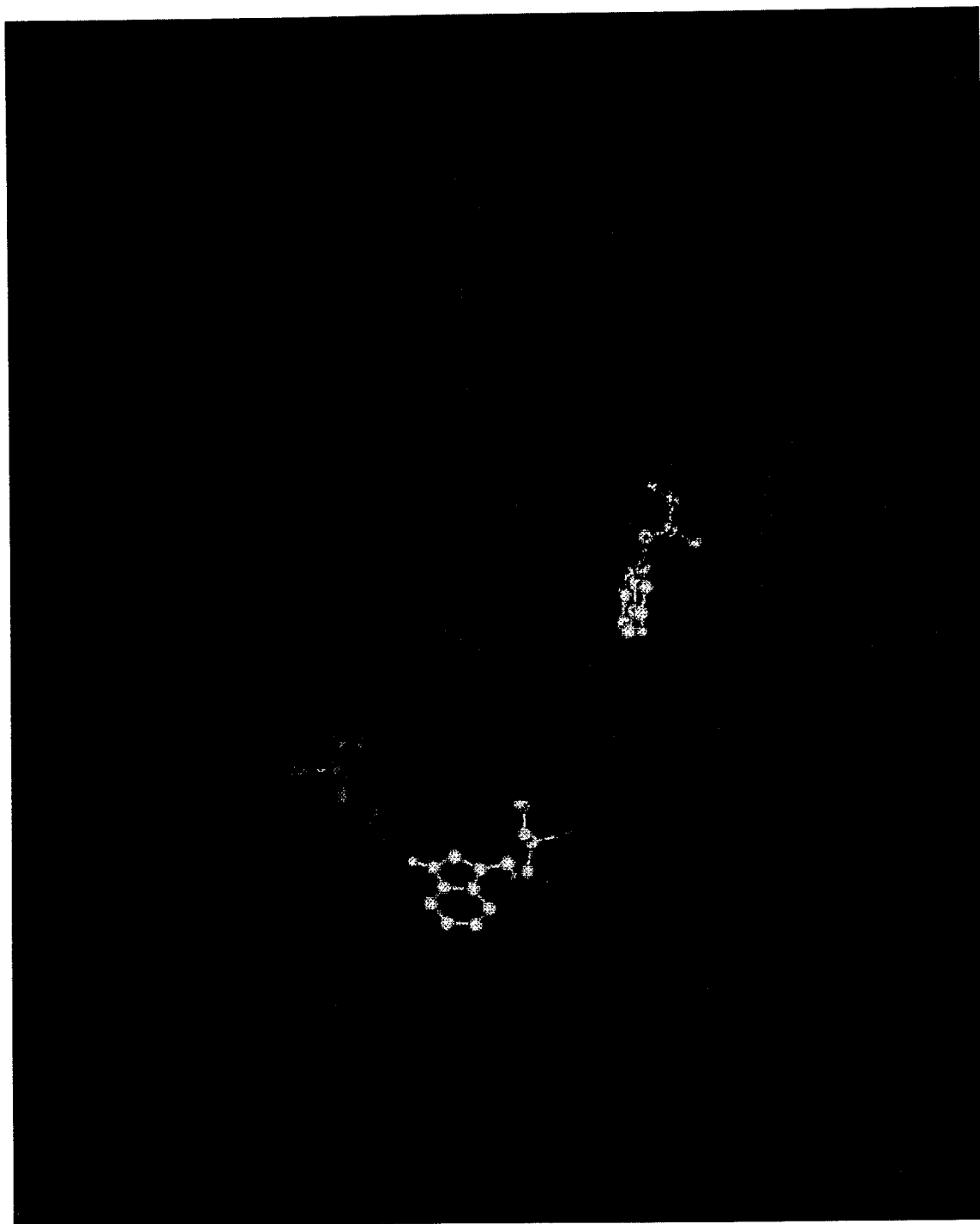


**Figure 13.** Cross section through the active-site gorge of AChE. The molecular surface is shown in lavender, and electrostatic field vectors are shown in green. The catalytic triad residues, Ser-200, Glu-327 and His-440 are shown in yellow, orange, and red, respectively. Trp-279, at top of the gorge, and Trp-84, adjacent to the triad, are shown in white.

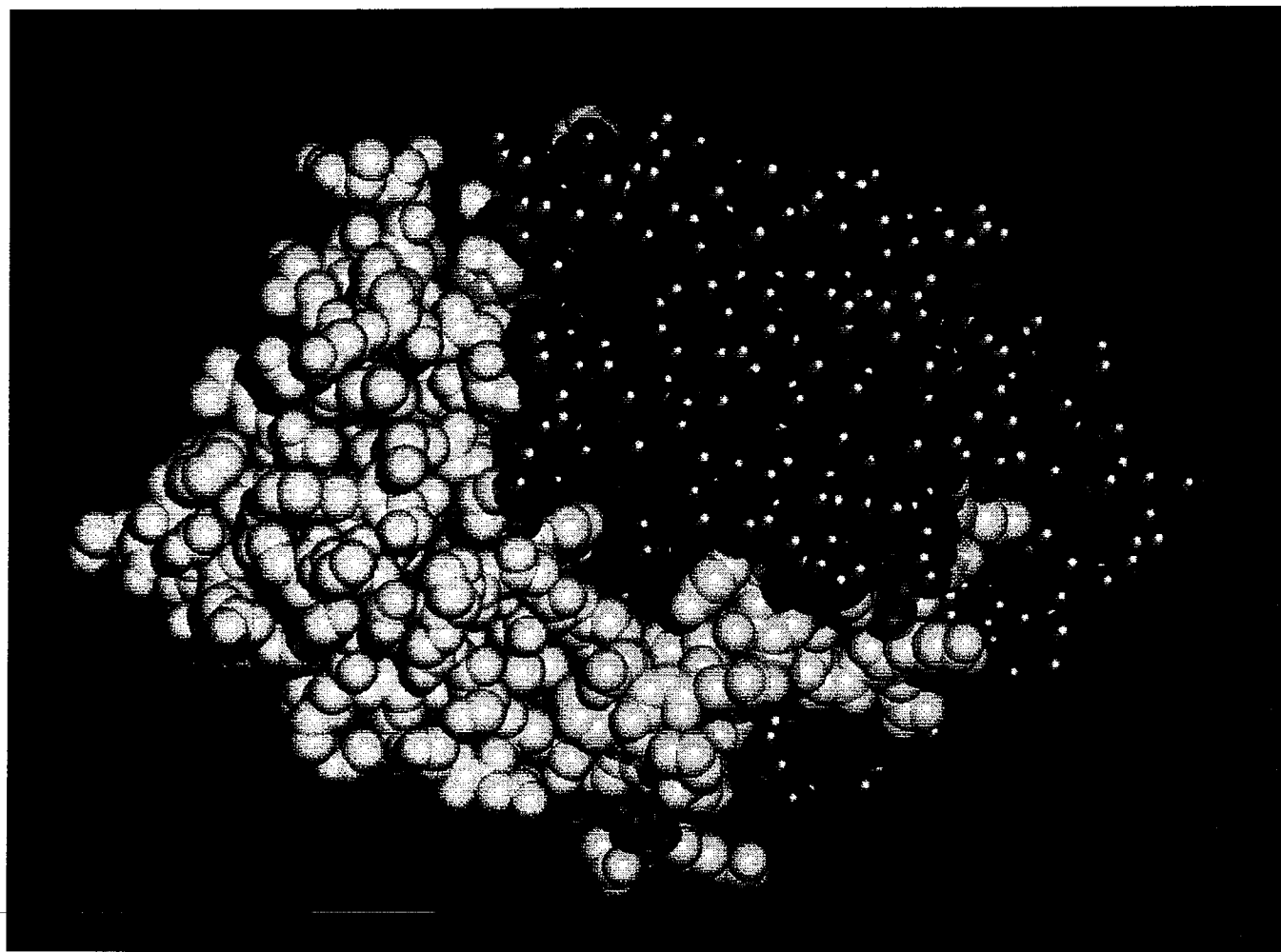


**Figure 14.** Ray-trace image of the active-site gorge of *Torpedo* AChE. The gorge opening is viewed directly down the gorge axis. N-terminal residues 4-310 are in blue, except for residues 67-94 (white), which represent the thin wall. Residues 311-534 are in yellow, and a molecule of DECA in the gorge is in red. Image generated with the program QUANTA.

## V REFERENCES:

1. Neuromuscular Transmission - Enzymatic Destruction of Acetylcholine (1974), Barnard, E. A., In *The Peripheral Nervous System* (J.I. Hubbard, Eds.), pp. 201-224, Plenum, New York.
2. Acetylcholinesterase: Enzyme Structure, Reaction Dynamics, and Virtual Transition States (1987), Quinn, D. M., *Chem. Rev.*, **87**, 955-975.
3. Cholinesterase and Anti-cholinesterase Agents (1963), Koelle, G. B., Eds., Springer-Verlag, Heidelberg.
4. Enzyme Inhibitors as Substrates, (1972), Aldridge, W. N. and Reiner, E., North Holland, Amsterdam.
5. Anticholinesterase Agents (1990), Taylor, P., In *The Pharmacological Basis of Therapeutics, 5th edition* (A.G. Gilman, A.S. Nies, T.W. Rall and P. Taylor, Eds.), pp. 131-150, MacMillan, New York.
6. Cholinergic Basis for Alzheimer Therapy (1991), Becker, R. E. and Giacobini, E., Eds., Birkhauser, Boston.
7. Acetylcholine Binding by a Synthetic Receptor: Implications for Biological Recognition (1990), Dougherty, D. A. and Stauffer, D. A., *Science*, **250**, 1558-1560.
8. Nicotinic Acetylcholine Receptor at 9 Å Resolution (1993), Unwin, N., *J. Mol. Biol.*, **229**, 1101-1124.
9. Atomic Structure of Acetylcholinesterase from *Torpedo californica*: A Prototypic Acetylcholine-Binding Protein (1991), Sussman, J. L., Harel, M., Frolow, F., Oefner, C., Goldman, A., Toker, L. and Silman, I., *Science*, **253**, 872-879.
10. Crystallographic and NMR Studies of the Serine Proteases (1982), Steitz, T. A. and Shulman, R. G., *Ann. Rev. Biophys. Bioeng.*, **11**, 419-444.

11. Structure and Dynamics of the Active Site Gorge of Acetylcholinesterase: Synergistic Use of Molecular Dynamics Simulation and X-ray Crystallography (1994), Axelsen, P. H., Harel, M., Silman, I. and Sussman, J. L., *Prot. Sci.*, **3**, 188-197.
12. Effective Charge on Acetylcholinesterase Active Sites Determined from the Ionic Strength Dependence of Association Rate Constants with Cationic Ligands (1980), Nolte, H.-J., Rosenberry, T. L. and Neumann, E., *Biochemistry*, **19**, 3705-3711.
13. Quaternary Ligand Binding to Aromatic Residues in the Active-site Gorge of Acetylcholinesterase (1993), Harel, M., Schalk, I., Ehret-Sabatier, L., Bouet, F., Goeldner, M., Hirth, C., Axelsen, P., Silman, I. and Sussman, J. L., *Proc. Natl. Acad. Sci. USA*, **90**, 9031-9035.
14. Anionic Subsites of the Acetylcholinesterase from *Torpedo californica*: Affinity Labelling with the Cationic Reagent *N,N*-Dimethyl-2-phenyl-aziridinium (1990), Weise, C., Kreienkamp, H.-J., Raba, R., Pedak, A., Aaviksaar, A. and Hucho, F., *EMBO J.*, **9**, 3885-3888.
15. Alignment of Amino Acid Sequences of Acetylcholinesterases and Butyrylcholinesterases (1991), Gentry, M. K. and Doctor, B. P., In *Cholinesterases: Structure, Function, Mechanism, Genetics and Cell Biology* (J. Massoulié, F. Bacou, E. Barnard, A. Chatonnet, B.P. Doctor and D.M. Quinn, Eds.), pp. 394-398, American Chemical Society, Washington, DC.
16. A Model of Butyrylcholinesterase Based on the X-ray Structure of Acetylcholinesterase Indicates Differences in Specificity (1992), Harel, M., Silman, I. and Sussman, J. L., In *Multidisciplinary Approaches to Cholinesterase Functions* (A. Shafferman and B. Velan, Eds.), pp. 189-194, Plenum Press, New York.
17. The Inhibitory Effect of Stilbamidine, Curare and Related Compounds and its Relationship to the Active Groups of Acetylcholine Esterase. Action of Stilbamidine Upon Nerve Impulse Conduction (1950), Bergmann, F., Wilson, I. B. and Nachmansohn, D., *Biochim. Biophys. Acta*, **6**, 217-224.
18. Ligand Binding Properties of Acetylcholinesterase Determined with Fluorescent Probes (1974), Mooser, G. and Sigman, D. S., *Biochemistry*, **13**, 2299-2307.



19. Interaction of Fluorescence Probes with Acetylcholinesterase. The Site and Specificity of Propidium (1975), Taylor, P. and Lappi, S., *Biochemistry*, **14**, 1989-1997.
20. Role of the Peripheral Anionic Site on Acetylcholinesterase: Inhibition by Substrates and Coumarin Derivatives (1991), Radic, Z., Reiner, E. and Taylor, P., *Mol. Pharmacol.*, **39**, 98-104.
21. Three distinct domains distinguish between acetylcholinesterase and butyrylcholinesterase substrate and inhibitor specificities (1993), Radic, Z., Pickering, N., Vellom, D. C., Camp, S. and Taylor, P., *FASEB J.*, **7**, A1067.
22. Dissection of the Human Acetylcholinesterase Active Center - Determinants of Substrate Specificity - Identification of Residues Constituting the Anionic Site, The Hydrophobic Site, and the Acyl Pocket (1993), Ordentlich, A., Barak, D., Kronman, C., Flashner, Y., Leitner, M., Segall, Y., Ariel, N., Cohen, S., Velan, B. and Shafferman, A., *J. Biol. Chem.*, **268**, 17083-17095.
23. Differential Effects of "Peripheral" Site Ligands on *Torpedo* and Chicken Acetylcholinesterase (1994), Eichler, J., Anselmet, A., Sussman, J. L., Massoulié, J. and Silman, I., *Mol. Pharmacol.*, **45**, 335-340.
24. Substrate inhibition of Acetylcholinesterase: Residues Affecting Signal Transduction from the Surface to the Catalytic Center (1992), Shafferman, A., Velan, B., Ordentlich, A., Kronman, C., Grosfeld, H., Leitner, M., Flashner, Y., Cohen, S., Barak, D. and Ariel, N., *EMBO J.*, **11**, 3561-3568.
25. Modelling and Mutagenesis of Butyrylcholinesterase Based on the X-ray Structure of Acetylcholinesterase (1992), Silman, I., Harel, M., Krejci, E., Bon, S., Chanal, P., Sussman, J. L. and Massoulié, J., In *Membrane Proteins: Structures, Interactions and Models* (A. Pullman, J. Jortner and B. Pullman, Eds.), pp. 177-184, Kluwer Academic Publishers, Dordrecht, Holland.
26. Conversion of Acetylcholinesterase to Butyrylcholinesterase: Modeling and Mutagenesis (1992), Harel, M., Sussman, J. L., Krejci, E., Bon, S., Chanal, P., Massoulié, J. and Silman, I., *Proc. Natl. Acad. Sci. USA*, **89**, 10827-10831.

27. Compilation of Evaluated Mutants of Cholinesterases (1995), Shafferman, A., Kronman, C. and Ordentlich, A., In *Enzymes of the Cholinesterase Family* (A.L. Balasubramanian, B.P. Doctor, P. Taylor and D.M. Quinn, Eds.), pp. 481-488, Plenum Press, New York.
28. Three Distinct Domains in the Cholinesterase Molecule Confer Selectivity for Acetylcholinesterase and Butyrylcholinesterase (1993), Radic, Z., Pickering, N. A., Vellom, D. C., Camp, S. and Taylor, P., *Biochemistry*, **32**, 12074-12084.
29. Amino Acid Residues Controlling Acetylcholinesterase and Butyrylcholinesterase Specificity (1993), Vellom, D. C., Radic, Z., Li, Y., Pickering, N. A., Camp, S. and Taylor, P., *Biochemistry*, **32**, 12-17.
30. Identification of Covalently Bound Inositol in the Hydrophobic Membrane-Anchoring Domain of *Torpedo* Acetylcholinesterase (1985), Futerman, A. H., Low, M. G., Ackermann, K. E., Sherman, W. R. and Silman, I., *Biochem. Biophys. Res. Commun.*, **129**, 312-317.
31. Purification and Crystallization of a Dimeric Form of Acetylcholinesterase from *Torpedo californica* Subsequent to Solubilization with Phosphatidylinositol-specific Phospholipase C (1988), Sussman, J. L., Harel, M., Frolow, F., Varon, L., Toker, L., Futerman, A. H. and Silman, I., *J. Mol. Biol.*, **203**, 821-823.
32. The Hydrolytic Water Molecule in Trypsin, Revealed by Time-Resolved Laue Crystallography (1993), Singer, P. T., Smalås, A., Carty, R. P., Mangel, W. F. and Sweet, R. M., *Science*, **259**, 669-673.
33. Locating the Catalytic Water Molecule in Serine Proteases (1993), Singer, P. T., Smalås, A., Carty, R. P., Mangel, W. F. and Sweet, R. M., *Science*, **261**, 621-622.
34. *m*-(*N,N,N*-Trimethylammonio)trifluoroacetophenone: A Femtomolar Inhibitor of Acetylcholinesterase (1993), Nair, H. K., Lee, K. and Quinn, D. M., *J. Am. Chem. Soc.*, **115**, 9939-9941.

35. Molecular Recognition in Acetylcholinesterase Catalysis: Free-Energy Correlations for Substrate Inhibition and Turnover by Trifluoro Ketone Transition-State Analogs (1994), Nair, H. K., Seravalli, J., Arbuckle, T. and Quinn, D. M., *Biochemistry*, **33**, 8566-8576.
36. Fluorinated Aldehydes and Ketones Acting as Quasi-Substrate Inhibitors of Acetylcholinesterase (1979), Brodbeck, U., Schweikert, K., Gentinetta, R. and Rottenberg, M., *Biochim. Biophys. Acta*, **567**, 357-369.
37. Crystallographic *R* Factor Refinement by Molecular Dynamics (1987), Brünger, A. T., Kuriyan, J. and Karplus, M., *Science*, **235**, 458-460.
38. The Refined Crystal Structures of 'Aged' and 'Non-Aged' Organophosphoryl Conjugates of  $\gamma$ -Chymotrypsin (1991), Harel, M., Su, C. T., Frolow, F., Ashani, Y., Silman, I. and Sussman, J. L., *J. Mol. Biol.*, **221**, 909-918.
39. Molecular Cloning and Construction of the Coding Region for Human Acetylcholinesterase Reveals a G+C-rich Attenuating Structure (1990), Soreq, H., Ben-Aziz, R., Prody, C. A., Seidman, S., Gnatt, A., Neville, L., Lieman-Hurwitz, J., Lev-Lehman, E., Ginzberg, D., Lapidot-Lifson, Y. and Zakut, H., *Proc. Natl. Acad. Sci. USA*, **87**, 9688-9692.
40. Recombinant Human Acetylcholinesterase is Secreted from Transiently Transfected 293 Cells as a Soluble Globular Enzyme (1991), Velan, B., Kronman, C., Grosfeld, H., Leitner, M., Gozes, Y., Flashner, Y., Sery, T., Cohen, S., Ben-Aziz, R., Seidman, S., Shafferman, A. and Soreq, H., *Cell. Mol. Neurobiol.*, **11**, 143-156.
41. Production and Secretion of High-Levels of Recombinant Human Acetylcholinesterase in Cultured-Cell Lines - Microheterogeneity of the Catalytic Subunit C (1992), Kronman, C., Velan, B., Gozes, Y., Leitner, M., Flashner, Y., Lazar, A., Marcus, D., Sery, T., Papier, Y., Grosfeld, H., Cohen, S. and Shafferman, A., *Gene*, **121**, 295-304.
42. Expression and Reconstitution of Biologically-Active Human Acetylcholinesterase from *Escherichia coli* (1993), Fischer, M., Ittah, A., Leifer, I. and Gorecki, M., *Cell. Mol. Neurobiol.*, **13**, 25-38.
43. Intrinsic Forms of Acetylcholinesterase in Skeletal Muscle (1978), Silman, I., Lyles, J. M. and Barnard, E. A., *FEBS Lett.*, **94**, 166-170.

44. An Electrostatic Mechanism of Substrate Guidance Down the Aromatic Gorge of Acetylcholinesterase (1993), Ripoll, D. R., Faerman, C. H., Axelsen, P., Silman, I. and Sussman, J. L., *Proc. Natl. Acad. Sci. USA*, **90**, 5128-5132.
45. Energetics of Charge-Charge Interactions in Proteins (1988), Gilson, M. K. and Honig, B. H., *Proteins: Struct. Funct. Genetics*, **3**, 32-52.
46. Calculating Electrostatic Interactions in Bio-Molecules: Method and Error Assessment (1988), Gilson, M. K., Sharp, K. A. and Honig, B. H., *J. Comput. Chem.*, **9**, 327-335.
47. The  $\alpha/\beta$  Hydrolase Fold (1992), Ollis, D. L., Cheah, E., Cygler, M., Dijkstra, B., Frolow, F., Franken, S. M., Harel, M., Remington, S. J., Silman, I., Schrag, J., Sussman, J. L., Verschueren, K. H. G. and Goldman, A., *Protein Eng.*, **5**, 197-211.
48. Relationship Between Sequence Conservation and Three-dimensional Structure in a Large Family of Esterases, Lipases, and Related Proteins (1993), Cygler, M., Schrag, J. D., Sussman, J. L., Harel, M., Silman, I., Gentry, M. K. and Doctor, B. P., *Prot. Sci.*, **2**, 366-382.
49. Loops in Globular Proteins : A Novel Category of Secondary Structure (1986), Leszczynski, J. F. and Rose, G. D., *Science*, **234**, 849-855.
50. Two Conformational States of *Candida rugosa* Lipase (1994), Grochulski, P., Li, Y., Schrag, J. D. and Cygler, M., *Prot. Sci.*, **3**, 82-91.
51. Insights into Interfacial Activation from an Open Structure of *Candida rugosa* Lipase (1994), Grochulski, P., Li, Y., Schrag, J. D., Bouthillier, F., Smith, P., Harrison, D., Rubin, B. and Cygler, M., *J. Biol. Chem.*, **268**, 12843-12847.
52. Open "Back Door" in a Molecular Dynamics Simulation of Acetylcholinesterase (1994), Gilson, M. K., Straatsma, T. P., McCammon, J. A., Ripoll, D. R., Faerman, C. H., Axelsen, P., Silman, I. and Sussman, J. L., *Science*, **263**, 1276-1278.

53. The "Back Door" Hypothesis for Product Clearance in Acetylcholinesterase Challenged by Site-Directed Mutagenesis (1994), Kronman, C., Ordentlich, A., Barak, D., Velan, B. and Shafferman, A., *J. Biol. Chem.*, **269**, 27819-27822.